STAR: Efficient Preference-based Reinforcement Learning via Dual Regularization

Fengshuo Bai[1,2,3] **Rui Zhao**[4,*] **Hongming Zhang**[5] **Sijia Cui**[5] **Shao Zhang**[1]
Bo Xu[5] **Lei Han**[4,*] **Ying Wen**[1] **Yaodong Yang**[6,*]
[1]Shanghai Jiao Tong University [2]PKU-PsiBot Joint Lab [3]Zhongguancun Academy [4]Tencent
[5]National Key Laboratory of Cognition and Decision Intelligence for Complex Systems,
Institution of Automation, Chinese Academy of Sciences
[6]Institute for AI, Peking University

Abstract

Preference-based reinforcement learning (PbRL) bypasses complex reward engineering by learning from human feedback. However, due to the high cost of obtaining feedback, PbRL typically relies on a limited set of preference-labeled samples. This data scarcity introduces two key inefficiencies: (1) the reward model overfits to the limited feedback, leading to poor generalization to unseen samples, and (2) the agent exploits the learned reward model, exacerbating overestimation of action values in temporal difference (TD) learning. To address these issues, we propose STAR, an efficient PbRL method that integrates preference margin regularization and policy regularization. Preference margin regularization mitigates overfitting by introducing a bounded margin in reward optimization, preventing excessive bias toward specific feedback. Policy regularization bootstraps a conservative estimate $\widehat{Q}$ from well-supported state-action pairs in the replay memory, reducing overestimation during policy learning. Experimental results show that STAR improves feedback efficiency, achieving 34.8% higher performance in online settings and 29.7% in offline settings compared to state-of-the-art methods. Ablation studies confirm that STAR facilitates more robust reward and value function learning. The videos of this project are released at `https://sites.google.com/view/pbrl-star`.

1 Introduction

Reinforcement learning (RL) [47, 5] has demonstrated remarkable success across various domains [1, 66, 69, 35, 56, 26]. However, its reliance on well-designed reward functions remains a significant challenge, as defining rewards for complex tasks is often difficult [59, 39, 62]. For example, in robotic manipulation, re-orienting a cube with a dexterous hand requires quantifying intermediate states, which is non-trivial [3, 4, 58, 70].

Preference-based reinforcement learning (PbRL) offers an alternative by replacing explicit reward functions with human preferences over agent trajectories [24, 37, 28, 73, 57]. PbRL follows an iterative process: (1) collecting human feedback to train a reward model and (2) optimizing a policy using this learned reward model. This iterative process aligns the agent with human-desired behaviors without the need for manually specified dense reward signals.

Despite its advantages, PbRL suffers from two fundamental inefficiencies when human feedback is limited. First, the reward model tends to overfit due to the small amount of preference data, leading to poor generalization [13, 36, 60, 61, 54]. Second, policy learning exacerbates this issue: TD-based optimization relies on the learned reward model, and errors in reward estimation, combined

[*]Correspondence to: yaodong.yang@pku.edu.cn, leihan.cs@gmail.com, rui.zhao.ml@gmail.com.

with overestimated Q-value updates, cause unstable learning [13, 28, 64, 19]. These challenges are illustrated in Figure 1, which visualizes how reward overfitting and Q-value overestimation degrade PbRL performance. Similar issues have been discussed in prior work [28, 30], highlighting the need for more feedback-efficient solutions. Addressing these inefficiencies is crucial for making PbRL viable in real-world applications, where extensive human feedback is impractical.

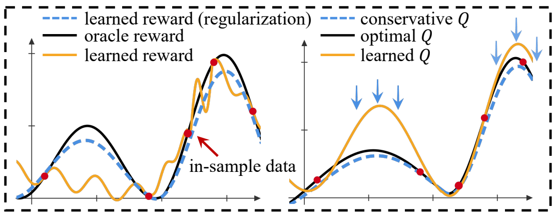

Figure 1: Illustration of two core inefficiencies—reward learning (left) and value estimation (right)—under limited human feedback. Our proposed STAR integrates preference regularization and conservative estimation to mitigate these challenges.

To address these challenges, we introduce STAR, a feedback-efficient PbRL algorithm that integrates two complementary techniques: human preference**S** margin regulariza**T**ion and policy regul**AR**ization. Preference regularization mitigates overfitting in reward learning by introducing a bounded margin in the optimization objective of standard preference learning, preventing the model from overly focusing on limited feedback data. Policy regularization reduces overestimation bias during RL training by estimating a conservative $\widehat{Q}$ value using only transitions stored in replay memory. This estimate is then used to constrain policy updates via Kullback-Leibler (KL) divergence, stabilizing learning. Our empirical evaluations across complex manipulation and locomotion tasks, in both online and offline PbRL settings, demonstrate that STAR consistently outperforms baselines. Notably, this advantage is particularly pronounced when human feedback is limited, highlighting STAR's ability to make efficient use of limited data for superior performance.

The key contributions of our work are as follows: (1) We propose STAR, a novel feedback-efficient PbRL algorithm that integrates preference margin regularization and policy regularization to improve learning stability and feedback utilization. (2) We demonstrate that STAR enhances feedback efficiency over existing PbRL methods across diverse online and offline tasks. Furthermore, human experiments reveal the emergence of novel behaviors driven by human feedback. (3) We provide in-depth analysis showing that preference margin regularization and policy regularization improve the accuracy of the reward model and mitigate Q-value overestimation, leading to improved policy optimization in feedback-limited settings.

2 Related Work

Preference-based Reinforcement Learning. PbRL is a novel way to learn agents from human feedback without reward engineering. Instead, a human provides preferences between the agent's behaviors, and the agent uses this feedback to perform the task. Christiano et al. [4] formulates a basic framework, and Ibarz et al. [17] utilizes imitation learning as the warm-start strategy to speed up PbRL. To further improve feedback efficiency, **PEBBLE** [24] replaces PPO [44] with SAC [11] to achieve data efficiency and combines unsupervised pre-training with the reward relabeling technique during learning. Building upon this foundation, Park et al. [37] introduces **SURF**, a semi-supervised reward learning framework that improves reward learning via pseudo-labels and temporal cropping augmentation. **MRN** [28] incorporates bi-level optimization for improving the quality of the Q function. **QPA** [16] improves feedback efficiency by addressing the issue of query-policy misalignment. Besides, some research has various considerations, such as skill extraction [55], intrinsic reward [27], meta-learning [14], and these methods have improved the efficiency to a certain extent. In addition to focusing on PbRL in online settings, a significant portion of research also concentrates on it in offline settings. **PT** [21] leverages a transformer architecture to learn a non-Markovian reward and preference weighting function. **IPL** [13] directly optimizes the implicit rewards deduced from the learned Q-function, ensuring alignment with expert preferences. Kang et al. [20] models offline trajectories and preferences in a one-step process without reward learning. **DTR** [51] balances staying close to the behavior policy with high-return trajectories and choosing actions with high reward labels. When dealing with language models, PbRL naturally facilitates the emergence of reinforcement learning from human feedback (RLHF) [36]. Before that, Stiennon et al. [45] have fine-tuned a summarizing policy following the PbRL paradigm. Our approach is orthogonal to previous approaches in that we use a conservative estimate $\widehat{Q}$ to regularize the neural Q-function to mitigate overestimation and leverage the preference margin regularization to prevent overfitting of the reward model.

3 Preliminaries

3.1 Preference-based Reinforcement Learning

In the preference-based RL framework, human preferences replace hand-craft rewards. Following the notation in Christiano et al. [4], a trajectory segment σ is defined as a sequence of states and actions $(s_{t+1}, a_{t+1}, \ldots, s_{t+k}, a_{t+k})$. Given a pair of segments (σ^0, σ^1), a human provides preference label y, which is a distribution over $\{(1,0),(0,1),(0.5,0.5)\}$ indicating preference for σ^0, σ^1, or indifference.

The reward model $\widehat{r}_\psi$ assigns scores to state-action pairs, and the cumulative reward over a segment is used to predict human preferences. Following the Bradley-Terry model [2], the preference predictor is formulated as:

$$P_\psi[\sigma^0 \succ \sigma^1] = \text{Sigmoid}\Big(\sum_t \widehat{r}_\psi(s_t^0, a_t^0) - \sum_t \widehat{r}_\psi(s_t^1, a_t^1)\Big), \tag{1}$$

where $\sigma^0 \succ \sigma^1$ indicates σ^0 is more consistent with human expectations than σ^1.

The reward model is optimized by minimizing the cross-entropy loss between predicted and actual preferences:

$$\mathcal{L}_{\text{reward}}(\psi) = -\mathop{\mathbb{E}}_{(\sigma^0,\sigma^1,y)\sim\mathcal{D}_{\text{pref}}}\Big[y(0)\log P_\psi[\sigma^0 \succ \sigma^1] + y(1)\log P_\psi[\sigma^1 \succ \sigma^0]\Big], \tag{2}$$

where $\mathcal{D}_{\text{pref}}$ denotes the dataset of preference pairs.

3.2 TD3-Based PbRL Framework

Twin Delayed Deep Deterministic Policy Gradient (TD3) [9] is an off-policy actor-critic algorithm designed to address value overestimation in deep reinforcement learning. When implementing PbRL with TD3, the learned reward model $\widehat{r}_\psi$ replaces the environment reward in the standard TD3 pipeline. The policy learning objective becomes maximizing :

$$\mathcal{J}_\pi(\phi) = \mathbb{E}_{s\sim\mathcal{D}}\left[\min_{j=1,2} Q_{\theta_j}(s, \pi_\phi(s))\right], \tag{3}$$

where $\mathcal{D}$ is the replay buffer of transition samples, and Q_{θ_j} is the j-th Q-function.

Each Q-function is trained to minimize the TD error with rewards from the learned model $\widehat{r}_\psi$:

$$\mathcal{J}_Q(\theta_j) = \mathbb{E}_{(s_t,a_t,s_{t+1})\sim\mathcal{D}}\left[\left(Q_{\theta_j}(s_t,a_t) - y_t\right)^2\right], \tag{4}$$

where the target value $y_t = \widehat{r}_\psi(s_t,a_t) + \gamma \min_{j'=1,2} Q_{\bar{\theta}_{j'}}(s_{t+1}, \pi_{\bar{\phi}}(s_{t+1}) + \epsilon)$. Here, $\bar{\theta}$ and $\bar{\phi}$ denote the target networks for Q-functions and policy; $\gamma \in [0,1)$ is the discount factor; and $\epsilon \sim \text{clip}(\mathcal{N}(0,\sigma), -c, c)$ is the clipped noise added for target policy smoothing.

4 Method

In this section, we introduce STAR, a flexible framework designed to enhance feedback efficiency in any PbRL approach. Figure 2 provides an overview of our method, which build up dual regularization through three core components: preference regularization, conservative value estimation ($\widehat{Q}$), and policy regularization. These components work together to optimize feedback utilization and improve policy performance. The detailed procedures for both the online and offline settings are outlined in Algorithms 1 and 2 in Appendix A.

4.1 Preference Regularization with Bounded Margin

Intuition and Analysis. We analyze the issue of reward over-optimization in preference-based learning. As discussed in Section 3.1, optimizing Equation (2) encourages the reward model to align with human preferences. However, this objective implicitly drives the optimization toward an unbounded reward difference between preferred and rejected segments: $\sum_t \widehat{r}_\psi(s_t^0, a_t^0) - \sum_t \widehat{r}_\psi(s_t^1, a_t^1) \to \infty$. Although the predicted rewards do not become literally infinite in practice, this unbounded optimization tendency indicates that Equation (2) is an ill-posed objective. It encourages the model to become overconfident in its predictions for training data, leading to poor generalization and the reward over-optimization problem. To address this, we introduce Preference Margin Regularization

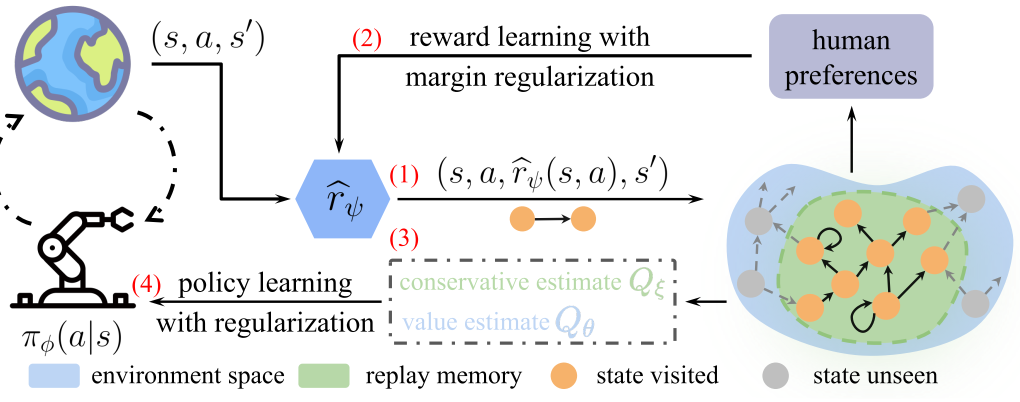
(s, a, s')
(2) reward learning with margin regularization
human preferences
$\widehat{r}_\psi$
(1) $(s, a, \widehat{r}_\psi(s,a), s')$
(3)
conservative estimate Q_ξ
value estimate Q_θ
(4) policy learning with regularization
$\pi_\phi(a|s)$
environment space
replay memory
state visited
state unseen

Figure 2: **Illustration of STAR.** (1) Label rewards using $\widehat{r}_\psi$. (2) Update the reward model $\widehat{r}_\psi$ via a bounded optimization objective from preference margin regularization. (3) Estimate conservative Q_ξ and update Q_θ. (4) Regularize π_ϕ with Q_ξ.

(PMR), which enforces a more reasonable decision boundary between preferred and rejected segments, thereby mitigating overfitting to training preferences. Detailed derivations and analyses are provided in Appendix B.1.

PMR Formulation. Drawing from margin learning theory [43, 46, 29], we propose PMR, which introduces a margin parameter ε to smooth the target distribution:

$$y_{\text{smooth}} = (1-\varepsilon)\cdot y + \varepsilon \cdot (1-y). \tag{5}$$

The PMR loss function becomes:

$$\mathcal{L}_{\text{PMR}}(\psi) = -\mathop{\mathbb{E}}_{(\sigma^0,\sigma^1,y)\sim\mathcal{D}}\Big[\sum_{i=0}^{1} y_{\text{smooth}}(i)\log P_\psi[\sigma^i \succ \sigma^{1-i}]\Big]. \tag{6}$$

By setting the derivative of this loss to zero and solving for the optimal solution, we can show that PMR implicitly enforces a bounded margin:

$$\sum_t \widehat{r}_\psi(s_t^0, a_t^0) - \sum_t \widehat{r}_\psi(s_t^1, a_t^1) = \log\left(\frac{1-\varepsilon}{\varepsilon}\right). \tag{7}$$

This bounded margin between preferred and rejected samples replaces the unbounded optimization objective of standard preference learning, effectively preventing the reward model from becoming overly confident while maintaining sufficient discriminative power.

4.2 Policy Regularization with Conservative Q

Building upon our analysis of reward overfitting, we now address the complementary problem of Q-function overestimation in PbRL. Even with a well-calibrated reward model from PMR, standard Q-learning can still lead to overestimation, especially in regions with limited data.

Conservative Estimate Q_ξ. We introduce a conservative Q-function Q_ξ that only utilizes well-supported state-action pairs from the current replay memory. This conservative estimation provides two main advantages: firstly, it enables further exploitation of samples in the replay memory; secondly, it prevents overestimation caused by extrapolation in unseen states and actions. Following principles from conservative Q-learning [23, 22, 10, 67, 68], we define a constrained operator $\mathcal{T}$:

$$\mathcal{T}^\beta Q_\xi(s_t, a_t) = \beta \log \mathbb{E}_{(s_t,a_t)\sim\mathcal{D}}\left[\frac{1}{\beta}\exp(Q_\xi(s_t,a_t))\right], \tag{8}$$

where $\beta > 0$ is a temperature parameter. Since state-action pairs are sampled from the replay buffer, the operator focuses exclusively on in-distribution actions. For any $\beta_1 > \beta_2 > 0$, we have $\mathcal{T}^{\beta_1}Q_\xi < \mathcal{T}^{\beta_2}Q_\xi$. As $\beta \to \infty$, $\mathcal{T}^\beta Q_\xi \to \mathbb{E}[Q_\xi]$, while $\beta \to 0$ recovers the in-distribution greedy estimate, i.e., $\mathcal{T}^\beta Q_\xi \to \sup(Q_\xi)$.

The conservative Q-function Q_ξ is trained by minimizing:

$$\mathcal{J}_Q(\xi) = \mathbb{E}_{\tau_t^{\text{in}} \sim \mathcal{D}} \left[\left(Q_\xi(s_t, a_t) - \widehat{r}_\psi(s_t, a_t) - \gamma \mathcal{T}^\beta Q_\xi(s_{t+1}, a_{t+1}) \right)^2 \right], \tag{9}$$

where in-distribution transition defined as: $\tau_t^{\text{in}} = (s_t, a_t, s_{t+1}, a_{t+1})$.

Policy Regularization. We leverage the conservative Q-function Q_ξ to regularize the policy learning process. The key insight is to use Q_ξ to derive a reference policy $\widehat{\pi}$ that captures the current best estimate of action distributions given uncertainty: $\widehat{\pi}(a|s) \propto \exp(Q_\xi(s,a))/Z(s)$, where $Z(s)$ is the partition function ensuring normalization.

We regularize the learned policy π_ϕ toward this reference policy using the KL divergence. Combined with the TD3 policy loss in Equation (3), the overall objective becomes:

$$\mathcal{J}_\pi(\phi) = \mathbb{E}_{s_t \sim \mathcal{D}} \Big[Q_\theta(s_t, \pi_\phi(s_t)) + \eta D_{\text{KL}} \left(\pi_\phi(\cdot|s_t) \| \widehat{\pi}(\cdot|s_t) \right) \Big], \tag{10}$$

where $\eta > 0$ controls the regularization strength. This formulation ensures that the policy optimization is guided by both the current Q-function Q_θ and the conservative estimate Q_ξ.

4.3 Theoretical Analysis

We provide a theoretical analysis to show the properties of the conservative estimate, denoted as $\widehat{Q}$, in a finite state-action space $\mathcal{S} \times \mathcal{A}$. Unlike the standard Q-function Q, which bootstraps over the entire action space, $\widehat{Q}$ bootstraps only in-distribution actions, thereby reducing extrapolation error from out-of-distribution data. As a result, $\widehat{Q}$ provides a conservative (i.e., lower-bound) estimate of Q, and converges to the optimal value as data coverage increases. The proof of the following theorem is provided in Appendix B.2.

Theorem 4.1. *Consider a tabular setting with finite state-action space $\mathcal{S} \times \mathcal{A}$. Let Q_t and $\widehat{Q}_t$ denote the Q-values at iteration t, updated via the standard Bellman optimality equation and the in-distribution bootstrapping variant, respectively. Then, both sequences converge to fixed points Q^* and $\widehat{Q}^*$, i.e., $\lim_{t\to\infty} Q_t = Q^*$ and $\lim_{t\to\infty} \widehat{Q}_t = \widehat{Q}^*$. Furthermore, for all $(s,a) \in \mathcal{S} \times \mathcal{A}$, we have $\widehat{Q}^*(s,a) \leq Q^*(s,a)$, with equality holding if all state-action pairs are visited.*

5 Experiments

We design our experiments to evaluate the effectiveness of STAR under various conditions and to validate the impact of our key design components. Specifically, we aim to answer the following questions: $\mathcal{Q}1$: Does STAR achieve strong performance with limited feedback in both online and offline settings? (Sec. 5.3) $\mathcal{Q}2$: Can preference regularization mitigate overfitting in the reward model? (Sec. 5.4) $\mathcal{Q}3$: Does policy regularization alleviate Q-value overestimation compared to prior methods? (Sec. 5.4) $\mathcal{Q}4$: How do the two regularization components complement each other to improve overall learning efficiency? (Sec. 5.4)

Further details about the tasks used in our experiments are provided in Appendix D.

5.1 Evaluation Setup

Tasks. We evaluate STAR on **18 tasks** drawn from standard benchmarks. In the online setting, we use three locomotion tasks from the DeepMind Control Suite (DMControl) [52] and three robotic manipulation tasks from Meta-World [63, 65]. For the offline setting, we include eight challenging control tasks from D4RL [7] and four robotic manipulation tasks from Robosuite [74]. These tasks span a diverse set of continuous control scenarios, varying in complexity and feedback characteristics.

Baselines. We compare STAR against several state-of-the-art methods, covering both online and offline PbRL settings. **Online Methods:** (1) *PEBBLE*[24]: combines unsupervised pretraining with reward relabeling to improve sample efficiency during policy learning. (2) *SURF*[37]: employs temporal data augmentation and pseudo-labels in a semi-supervised framework to enhance policy performance. (3) *MRN* [28]: introduces bi-level optimization for reward learning and represents the current state-of-the-art in online PbRL. **Offline Methods:** (4) *PT*[21]: leverages transformer-based architectures to model non-Markovian rewards and preference-weighting functions, capturing long-term dependencies in offline PbRL. (5) *IPL*[13]: directly optimizes implicit rewards derived from the learned Q-function to align with expert preferences. (6) *DTR*[51]: balances staying close

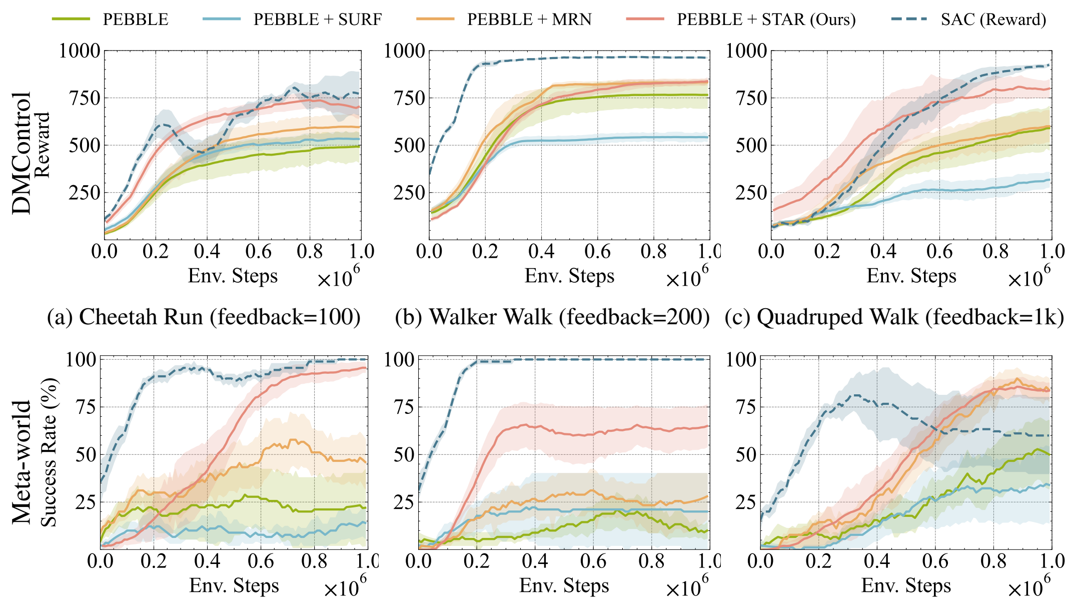

(a) Cheetah Run (feedback=100) (b) Walker Walk (feedback=200) (c) Quadruped Walk (feedback=1k)

(d) Button Press (feedback=100) (e) Window Open (feedback=100) (f) Sweep Into (feedback=4k)

Figure 3: Evaluating curves of all methods on locomotion tasks and robotic manipulation tasks. The solid line presents the mean values, while the shaded area indicates the 78% confidence interval over five runs. The red line is our method.

to the behavior policy with high-return trajectories and choosing actions with high reward labels. **Reward-based Methods:** Since PbRL lacks explicit rewards, we also report results from reward-based algorithms for reference. For online settings, we include (7) *SAC*[11]; for offline settings, we evaluate (8) *IQL*[22] and (9) *TD3+BC* [8]. These comparisons provide a reference for evaluating the performance of STAR relative to methods with access to ground-truth rewards.

Evaluation Metrics. We evaluate all algorithms over five independent trials per task and report the mean and standard deviation of their performance. Meta-World tasks (Button Press, Window Open and Sweep Into) are assessed using *success rate*, as they involve goal-conditioned objectives, while DMControl tasks (Cheetah Run, Walker Walk and Quadruped Walk) and offline benchmarks are evaluated based on *ground-truth episode return*, which captures cumulative performance in continuous control settings.

5.2 Implementation details

In our experiments, we follow the basic setup employed by prior work [24, 37, 28], which includes unsupervised exploration and an uncertainty-based trajectory sampling strategy. All methods employ an ensemble of three reward models, with outputs bounded in $[-1, 1]$ using a hyperbolic tangent activation (details in Appendix C.1).

To enable systematic and reproducible evaluation, we adopt a scripted teacher, following [24, 37, 28], which generates preference labels by comparing pairs of trajectory segments based on the environment's true reward function. These preferences accurately reflect the underlying rewards, enabling direct quantitative comparison across algorithms. Importantly, agents do not have access to ground-truth rewards and rely solely on preference signals. For offline experiments, we use real human preference data from Kim et al. [21]. The number of preference pairs varies by task complexity: 100 pairs for tasks such as Cheetah Run, Button Press, and Window Open; 500 pairs for tasks like Hopper-medium-replay-v2; and up to 4000 pairs for more complex tasks like Sweep Into. The number of preference labels used per task is detailed in Appendix C.2.

To ensure fair comparisons, all methods are trained with the same network architecture and shared hyperparameters, including learning rate and batch size. The only differences lie in method-specific components such as the loss function. We use publicly available implementations for PEBBLE, SURF, MRN, and IPL. Additional implementation details, including hyperparameter settings and network architecture, are provided in Appendix C.

5.3 Main Results

Our evaluation primarily focuses on training with limited feedback. This refers to an insufficient number of preference labels compared to the feedback required to achieve SAC algorithm performance.

Online Settings. We evaluate STAR's performance on three locomotion tasks from DMControl and three robotic manipulation tasks from Meta-World. As shown in Figure 3, STAR outperforms the baselines in most tasks. In the Cheetah Run task, STAR achieves 96% of the best performance using only 100 preference labels, demonstrating efficient feedback usage. Building on PEBBLE as the backbone, the comparison between the red (STAR) and green (PEBBLE) curves in Figure 3 reveals a significant performance gap. This highlights the effectiveness of our techniques, including preference margin regularization and policy regularization, in enhancing performance with limited preference labels.

Table 1: **Summary of normalized scores.** Mean normalized scores (baseline / SAC) across tasks from DMControl and Meta-World.

Task/Method	PEBBLE	SURF	MRN	STAR (ours)
DMControl	0.704	0.550	0.781	0.881
Meta-world	0.358	0.309	0.614	1.000
Average	0.531	0.430	0.698	0.941 (**34.8%** $\uparrow$)

Table 2: Averaged normalized scores of all baselines on AntMaze, Gym-Mujoco locomotion tasks, and success rate on Robosuite tasks. All agents training use the same real human preferences dataset from Kim et al. [21]. We train the STAR and IPL, and report the average and standard deviation averaged over 15 episodes. The term 'reward' refers to the use of ground-truth rewards.

Dataset	IQL (reward)	TD3+BC (reward)	MR	PT	IPL	DTR	STAR (ours)
antmaze-medium-play-v2	73.88 $\pm$ 4.49	0.25 $\pm$ 0.43	31.13 $\pm$ 16.96	70.13 $\pm$ 3.76	30.19 $\pm$ 4.97	67.12 $\pm$ 4.22	69.0 $\pm$ 14.97
antmaze-medium-diverse-v2	68.13 $\pm$ 10.15	0.25 $\pm$ 0.43	19.38 $\pm$ 9.24	65.25 $\pm$ 3.59	24.21 $\pm$ 5.12	63.23 $\pm$ 15.19	67.0 $\pm$ 17.44
antmaze-large-play-v2	48.75 $\pm$ 4.35	0.0 $\pm$ 0.0	24.25 $\pm$ 14.03	42.38 $\pm$ 9.98	12.46 $\pm$ 7.2	45.93 $\pm$ 14.32	50.67 $\pm$ 10.2
antmaze-large-diverse-v2	44.38 $\pm$ 4.47	0.0 $\pm$ 0.0	5.88 $\pm$ 6.94	19.63 $\pm$ 3.70	0.0 $\pm$ 0.0	47.10 $\pm$ 12.31	48.0 $\pm$ 16.0
antmaze-v2 total	58.79	0.13	20.16	49.35	16.72	55.85	**58.67**
hopper-medium-replay-v2	83.06 $\pm$ 15.80	64.42 $\pm$ 21.52	11.56 $\pm$ 30.27	84.54 $\pm$ 4.07	73.57 $\pm$ 6.7	82.12 $\pm$ 21.38	85.29 $\pm$ 5.11
hopper-medium-expert-v2	73.55 $\pm$ 41.47	101.17 $\pm$ 9.07	57.75 $\pm$ 23.70	68.96 $\pm$ 33.86	74.52 $\pm$ 0.1	91.13 $\pm$ 27.20	96.75 $\pm$ 4.31
walker2d-medium-replay-v2	73.11 $\pm$ 8.07	85.62 $\pm$ 4.01	72.07 $\pm$ 1.96	71.27 $\pm$ 10.30	59.92 $\pm$ 5.1	73.00 $\pm$ 7.13	73.91 $\pm$ 1.33
walker2d-medium-expert-v2	107.75 $\pm$ 2.02	110.03 $\pm$ 0.36	108.32 $\pm$ 3.87	110.13 $\pm$ 0.21	108.51 $\pm$ 0.6	108.39 $\pm$ 5.28	110.12 $\pm$ 0.24
locomotion-v2 total	84.37	90.31	62.43	83.72	79.13	88.66	**91.52**
lift-ph	96.75 $\pm$ 1.83	-	84.75 $\pm$ 6.23	91.75 $\pm$ 5.90	97.6 $\pm$ 2.9	94.51 $\pm$ 3.67	98.0 $\pm$ 4.0
lift-mh	86.75 $\pm$ 2.82	-	91.00 $\pm$ 4.00	86.75 $\pm$ 5.95	87.2 $\pm$ 5.3	92.69 $\pm$ 4.81	93.0 $\pm$ 8.94
can-ph	74.50 $\pm$ 6.82	-	68.00 $\pm$ 9.13	69.67 $\pm$ 5.89	74.8 $\pm$ 2.4	67.12 $\pm$ 9.76	70.0 $\pm$ 13.56
can-mh	56.25 $\pm$ 8.78	-	47.50 $\pm$ 3.51	50.50 $\pm$ 6.48	57.6 $\pm$ 5.0	42.71 $\pm$ 9.78	47.0 $\pm$ 9.8
robosuite total	78.56	-	72.81	74.66	**79.3**	74.26	77.0

To further illustrate the results, we summarize the mean normalized scores (baseline score / SAC score) across tasks from DMControl and Meta-World in Table 1. It shows that STAR surpasses the state-of-the-art (MRN) by 34.8%, indicating STAR significantly improves the feedback efficiency of PbRL methods across a range of complex tasks.

Offline Settings. We benchmark STAR against several offline PbRL algorithms using the D4RL [7] and Robosuite [74] robotics datasets, incorporating real-human preference data from Kim et al. [21]. To avoid relying on out-of-sample actions, we extract the policy using advantage weighted regression [38, 53, 34]. Our evaluation includes comparisons with two state-of-the-art offline PbRL algorithms, IPL and PT, as well as two significant offline RL algorithms. Since TD3 serves as our foundational RL algorithm, we also present results from TD3 enhanced with Behavior Cloning (TD3+BC) [8].

Additionally, we compare different reward model architectures: MR (MLP-based), LSTM (LSTM-based), and PT (Transformer-based), corresponding to models proposed by Christiano et al. [4], Early et al. [6], and Kim et al. [21], respectively. The results in Table 2 show that STAR outperforms all baselines on most tasks. On D4RL, our method achieves an average performance improvement of 29.7% compared to state-of-the-art methods. Notably, it exhibits a clear advantage in challenging tasks such as antmaze-large, where it nearly matches the performance of IQL with task rewards and

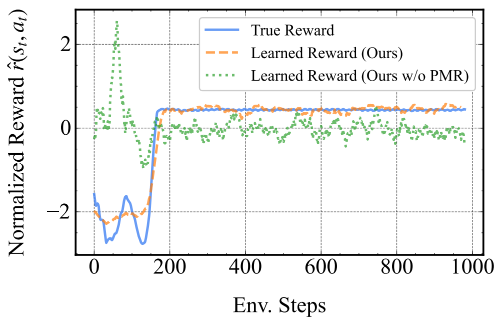

(a) Cheetah Run

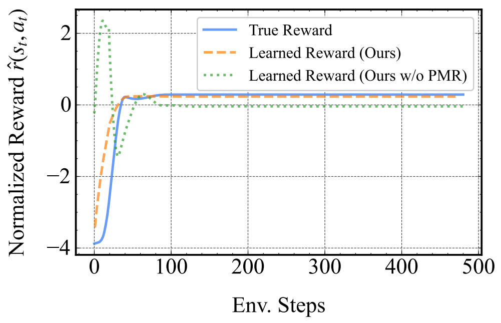

(b) Window Open

Figure 4: **Quality of Learned Reward.** Time series plots of the normalized learned reward (dashed line) and the ground-truth reward (solid line) obtained from rollouts of a policy trained with STAR.

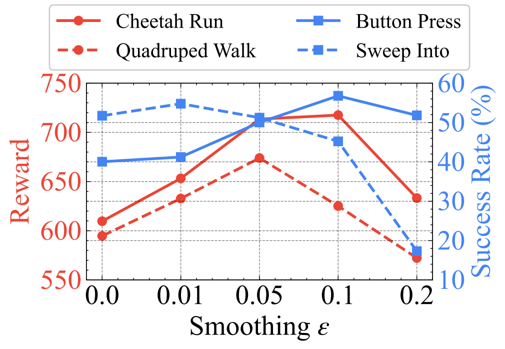

(a) Preference Regularization

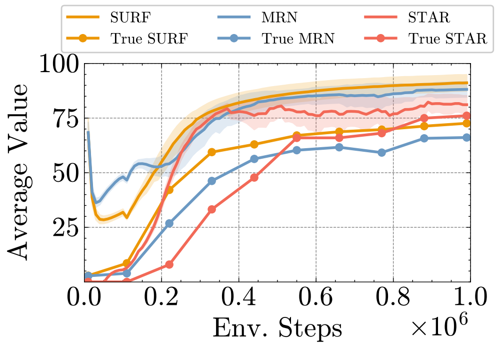

(b) Value Estimation Accuracy

Figure 5: Ablation studies evaluating (a) the impact of the parameter ε in preference margin regularization, and (b) the overestimation bias in value estimates.

even surpasses IQL in certain cases. These results highlight the effectiveness of our approach across diverse tasks in offline settings.

5.4 Ablation Studies

Quality of Learned Reward. To evaluate the impact of preference regularization on reward model quality, we compare the learned reward model with the ground-truth reward function on Cheetah Run and Window Open tasks. As shown in Figure 4, we plot time series curves for our method (STAR), its ablated variant without PMR, and the ground-truth reward. The results demonstrate that STAR produces a reward function that more closely tracks the ground-truth reward across time steps. In contrast, the variant without PMR exhibits higher variance and deviates significantly from the true reward, indicating that PMR contributes to improved reward model calibration.

Accuracy of Value Estimation. We assess the accuracy of value estimation in STAR by tracking the value estimate trajectory during the learning process on Cheetah Run. Figure 5b charts the average value estimate over 10,000 states and compares it to an estimate of the true value. The true value is computed as the average discounted return obtained by following the current policy using the ground truth reward. A clear overestimation bias is observed during learning, with SURF overestimating by 32% and MRN by 25%. When constrained by the policy regularizer, STAR significantly reduces overestimation bias to just 7%, leading to a more accurate Q-function. This reduction in bias directly improves value estimation, enabling a more stable and effective learning process in PbRL. Quantitatively, the overestimation error decreases by 72%, resulting in a more reliable learning trajectory and contributing to better policy performance across a variety of tasks.

Contribution of each technique. To assess the individual contributions of each technique and their interaction effects, we conduct an ablation study on preference margin regularization (PMR) and

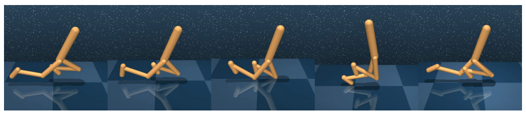
(a) Walker March

(b) Cheetah Prowl

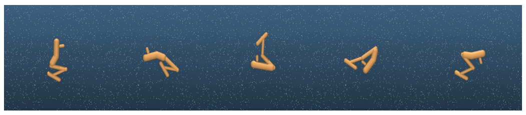
(c) Hopper Backflip

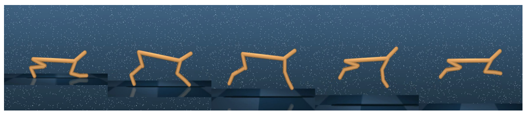
(d) Cheetah High Jump

Figure 7: **Human Experiments.** Novel skills learned from human feedback.

policy regularization (PR). Table 3 reports the performance on three tasks: Cheetah Run, Window Open, and Sweep Into. Removing either PMR or PR leads to a notable performance drop across all tasks, with the absence of both causing the most severe degradation. These results highlight that both techniques are essential and complementary in improving the robustness and effectiveness of STAR.

Table 3: **Contribution of Each Technique.** Performance on Cheetah Run is measured by episode return, while Window Open and Sweep Into are measured by success rate.

Task	Ours	Ours w/o PMR	Ours w/o PR	Ours w/o both
Cheetah Run	713.5	609.2	579.7	491.5
Window Open	65.0	50.0	41.2	10.0
Sweep Into	81.2	59.7	51.4	41.6

We further investigate the impact of the parameter ε in PMR. Figure 5a shows how varying ε influences the performance of STAR. Interestingly, even a small value (e.g., $\varepsilon = 0.01$) leads to noticeable performance gains, indicating the sensitivity of the reward model to minor regularization. However, excessively large ε values introduce estimation bias, consistent with observations in prior work [12, 33]. In addition, we observe that tasks with more feedback (e.g., Quadruped Walk, Sweep Into) tend to perform best with smaller ε values, whereas tasks with fewer feedback (e.g., Cheetah Run, Button Press) benefit from larger ε. This suggests that the severity of reward overfitting diminishes with increased feedback, reducing the need for aggressive smoothing.

Effect of Feedback Quantity. To further investigate how the number of feedback signals influences performance, we evaluate all methods on Walker Walk with varying amounts of feedback $N \in \{100, 200, 500, 1000\}$. As shown in Figure 6, performance improves across all methods as feedback increases, likely due to a more accurate reward model. Notably, STAR consistently outperforms all baselines, even under limited feedback, highlighting its ability to learn a more reliable Q-function and maintain strong performance with fewer preference labels.

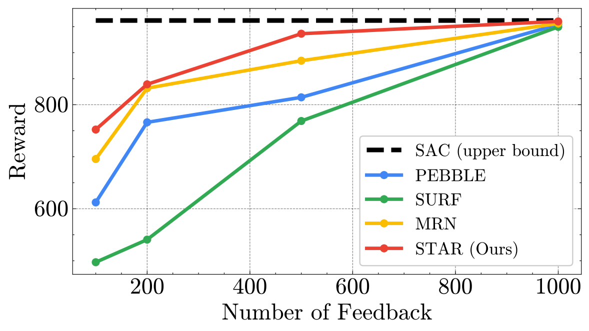

Figure 6: **Effect of Feedback Quantity on Walker.**

Human Experiments. We demonstrate that agents trained with STAR using human feedback can acquire novel and diverse skills, as illustrated in Figure 7. Specifically, we showcase: (a) a Walker lowering its center of gravity and marching, (b) a Cheetah agent prowling, (c) a Hopper performing a backflip, and (d) a Cheetah executing a high jump—each trained with only 50 human preference queries. These results underscore the effectiveness of human feedback in guiding complex behavior acquisition via STAR, particularly in settings where manual reward design is non-trivial. Videos of all behaviors are included in the supplementary material.

6 Conclusion

In this work, we introduce STAR, a novel preference-based RL algorithm that significantly enhances feedback efficiency. By integrating preference margin regularization and policy regularization, STAR outperforms prior methods and achieves strong performance across a range of complex tasks in both online and offline settings. A key strength of our method lies in its ability to learn effectively from a limited number of preference labels. Our analysis reveals two main factors driving this efficiency: **(1)** mitigating overestimation bias through conservative policy regularization, leading to more accurate Q-function estimates; and **(2)** reducing reward model overfitting via preference margin regularization. Additionally, human experiments demonstrate that STAR enables agents to acquire diverse and novel skills, reinforcing its practical potential. By improving the efficiency of PbRL, STAR takes a step toward making preference-driven learning more applicable to real-world robotic systems.

7 Limitation

Despite the significant improvement in feedback efficiency achieved by STAR, this work primarily focuses on state-based inputs. Extending the method to handle partially observable or high-dimensional inputs, such as raw RGB observations, remains an important direction for future research. Moreover, all experiments are conducted in simulation. A key next step for future is to investigate the applicability of STAR to real-world RL, enabling robots to acquire manipulation skills directly on physical platforms.

Acknowledgments

This work is partially supported by National Key R&D Program of China (2024YFC3505402) and Project No. 20240313, Zhongguancun Academy, Beijing, China (100094). We sincerely thank the anonymous reviewers for their helpful comments and suggestions, which improved this paper.

References

[1] Fengshuo Bai, Hongming Zhang, Tianyang Tao, Zhiheng Wu, Yanna Wang, and Bo Xu. Picor: Multi-task deep reinforcement learning with policy correction. 37(6):6728–6736, 2023.

[2] Ralph Allan Bradley and Milton E. Terry. Rank analysis of incomplete block designs: I. the method of paired comparisons. *Biometrika*, 39(3/4):324–345, 1952.

[3] Tao Chen, Jie Xu, and Pulkit Agrawal. A system for general in-hand object re-orientation. In *Conference on Robot Learning (CoRL)*, volume 164, pages 297–307. PMLR, 08–11 Nov 2022.

[4] Paul F Christiano, Jan Leike, Tom Brown, Miljan Martic, Shane Legg, and Dario Amodei. Deep reinforcement learning from human preferences. In *Advances in Neural Information Processing Systems (NeurIPS)*, volume 30, 2017.

[5] Hao Dong, Zihan Ding, and Shanghang Zhang. *Deep Reinforcement Learning: Fundamentals, Research and Applications*. Springer Nature, 2020.

[6] Joseph Early, Tom Bewley, Christine Evers, and Sarvapali Ramchurn. Non-markovian reward modelling from trajectory labels via interpretable multiple instance learning. In *Advances in Neural Information Processing Systems (NeurIPS)*, volume 35, pages 27652–27663, 2022.

[7] Justin Fu, Aviral Kumar, Ofir Nachum, George Tucker, and Sergey Levine. D4rl: Datasets for deep data-driven reinforcement learning. *arXiv preprint arXiv:2004.07219*, 2020.

[8] Scott Fujimoto and Shixiang (Shane) Gu. A minimalist approach to offline reinforcement learning. In *Advances in Neural Information Processing Systems (NeurIPS)*, volume 34, pages 20132–20145, 2021.

[9] Scott Fujimoto, Herke Hoof, and David Meger. Addressing function approximation error in actor-critic methods. In *International conference on machine learning (ICML)*, pages 1587–1596. PMLR, 2018.

[10] Divyansh Garg, Joey Hejna, Matthieu Geist, and Stefano Ermon. Extreme q-learning: Maxent RL without entropy. In *International Conference on Learning Representations (ICLR)*, 2023.

[11] Tuomas Haarnoja, Aurick Zhou, Pieter Abbeel, and Sergey Levine. Soft actor-critic: Off-policy maximum entropy deep reinforcement learning with a stochastic actor. In *International Conference on Machine Learning (ICML)*, volume 80, pages 1861–1870, 2018.

[12] Tong He, Zhi Zhang, Hang Zhang, Zhongyue Zhang, Junyuan Xie, and Mu Li. Bag of tricks for image classification with convolutional neural networks. In *IEEE/CVF conference on computer vision and pattern recognition (CVPR)*, pages 558–567, 2019.

[13] Joey Hejna and Dorsa Sadigh. Inverse preference learning: Preference-based RL without a reward function. In *Conference on Neural Information Processing Systems (NeurIPS)*, 2023.

[14] Donald Joseph Hejna III and Dorsa Sadigh. Few-shot preference learning for human-in-the-loop RL. In *International Conference on Robot Learning (CoRL)*, pages 2014–2025. PMLR, 2023.

[15] Zhang-Wei Hong, Tao Chen, Yen-Chen Lin, Joni Pajarinen, and Pulkit Agrawal. Topological experience replay. In *International Conference on Learning Representations (ICLR)*, 2022.

[16] Xiao Hu, Jianxiong Li, Xianyuan Zhan, Qing-Shan Jia, and Ya-Qin Zhang. Query-policy misalignment in preference-based reinforcement learning. In *International Conference on Learning Representations (ICLR)*, 2024.

[17] Borja Ibarz, Jan Leike, Tobias Pohlen, Geoffrey Irving, Shane Legg, and Dario Amodei. Reward learning from human preferences and demonstrations in atari. In *Advances in Neural Information Processing Systems (NeurIPS)*, volume 31, 2018.

[18] Tommi Jaakkola, Michael Jordan, and Satinder Singh. Convergence of stochastic iterative dynamic programming algorithms. *Advances in neural information processing systems (NeurIPS)*, 6, 1993.

[19] Xiaosong Jia, Zhenjie Yang, Qifeng Li, Zhiyuan Zhang, and Junchi Yan. Bench2drive: Towards multi-ability benchmarking of closed-loop end-to-end autonomous driving. *Advances in Neural Information Processing Systems (NeurIPS)*, 37:819–844, 2024.

[20] Yachen Kang, Diyuan Shi, Jinxin Liu, Li He, and Donglin Wang. Beyond reward: Offline preference-guided policy optimization. In *International Conference on Machine Learning (ICML)*, volume 202, pages 15753–15768, 23–29 Jul 2023.

[21] Changyeon Kim, Jongjin Park, Jinwoo Shin, Honglak Lee, Pieter Abbeel, and Kimin Lee. Preference transformer: Modeling human preferences using transformers for RL. In *International Conference on Learning Representations (ICLR)*, 2023.

[22] Ilya Kostrikov, Ashvin Nair, and Sergey Levine. Offline reinforcement learning with implicit q-learning. In *International Conference on Learning Representations (ICLR)*, 2022.

[23] Aviral Kumar, Aurick Zhou, George Tucker, and Sergey Levine. Conservative q-learning for offline reinforcement learning. In *Advances in Neural Information Processing Systems (NeurIPS)*, volume 33, pages 1179–1191, 2020.

[24] Kimin Lee, Laura M Smith, and Pieter Abbeel. Pebble: Feedback-efficient interactive reinforcement learning via relabeling experience and unsupervised pre-training. In *International Conference on Machine Learning (ICML)*, volume 139, pages 6152–6163, 2021.

[25] Su Young Lee, Choi Sungik, and Sae-Young Chung. Sample-efficient deep reinforcement learning via episodic backward update. In *Advances in Neural Information Processing Systems (NeurIPS)*, volume 32, 2019.

[26] Yang Li, Shao Zhang, Jichen Sun, Yali Du, Ying Wen, Xinbing Wang, and Wei Pan. Cooperative open-ended learning framework for zero-shot coordination. In *International Conference on Machine Learning*, pages 20470–20484. PMLR, 2023.

[27] Xinran Liang, Katherine Shu, Kimin Lee, and Pieter Abbeel. Reward uncertainty for exploration in preference-based reinforcement learning. In *International Conference on Learning Representations (ICLR)*, 2022.

[28] Runze Liu, Fengshuo Bai, Yali Du, and Yaodong Yang. Meta-reward-net: Implicitly differentiable reward learning for preference-based reinforcement learning. In *Advances in Neural Information Processing Systems (NeurIPS)*, volume 35, pages 22270–22284, 2022.

[29] Weiyang Liu, Yandong Wen, Zhiding Yu, and Meng Yang. Large-margin softmax loss for convolutional neural networks. In *International Conference on Machine Learning (ICML)*, pages 507–516, 2016.

[30] Long Ma, Yuanfei Wang, Fangwei Zhong, Song-Chun Zhu, and Yizhou Wang. Fast peer adaptation with context-aware exploration. *arXiv preprint arXiv:2402.02468*, 2024.

[31] Francisco S Melo. Convergence of q-learning: A simple proof. *Institute Of Systems and Robotics, Tech. Rep*, pages 1–4, 2001.

[32] Neeraj Misra, Harshinder Singh, and Vladimir Hnizdo. Nearest neighbor estimates of entropy. *American Journal of Mathematical and Management Sciences*, 23(3-4):301–321, 2003.

[33] Rafael Müller, Simon Kornblith, and Geoffrey E Hinton. When does label smoothing help? In *Advances in Neural Information Processing Systems (NeurIPS)*, volume 32, 2019.

[34] Ashvin Nair, Abhishek Gupta, Murtaza Dalal, and Sergey Levine. Awac: Accelerating online reinforcement learning with offline datasets. *arXiv preprint arXiv:2006.09359*, 2020.

[35] Yazhe Niu, Yuan Pu, Zhenjie Yang, Xueyan Li, Tong Zhou, Jiyuan Ren, Shuai Hu, Hongsheng Li, and Yu Liu. Lightzero: A unified benchmark for monte carlo tree search in general sequential decision scenarios. *Advances in Neural Information Processing Systems (NeurIPS)*, 36:37594–37635, 2023.

[36] Long Ouyang, Jeffrey Wu, Xu Jiang, Diogo Almeida, Carroll Wainwright, Pamela Mishkin, Chong Zhang, Sandhini Agarwal, Katarina Slama, Alex Ray, John Schulman, Jacob Hilton, Fraser Kelton, Luke Miller, Maddie Simens, Amanda Askell, Peter Welinder, Paul F Christiano, Jan Leike, and Ryan Lowe. Training language models to follow instructions with human feedback. In *Advances in Neural Information Processing Systems (NeurIPS)*, volume 35, pages 27730–27744, 2022.

[37] Jongjin Park, Younggyo Seo, Jinwoo Shin, Honglak Lee, Pieter Abbeel, and Kimin Lee. SURF: Semi-supervised reward learning with data augmentation for feedback-efficient preference-based reinforcement learning. In *International Conference on Learning Representations (ICLR)*, 2022.

[38] Jan Peters and Stefan Schaal. Reinforcement learning by reward-weighted regression for operational space control. In *International Conference on Machine Learning (ICML)*, page 745–750, 2007.

[39] Yuan Pu, Yazhe Niu, Zhenjie Yang, Jiyuan Ren, Hongsheng Li, and Yu Liu. Unizero: Generalized and efficient planning with scalable latent world models. *arXiv preprint arXiv:2406.10667*, 2024.

[40] Herbert Robbins and Sutton Monro. A stochastic approximation method. *The annals of mathematical statistics*, pages 400–407, 1951.

[41] Egor Rotinov. Reverse experience replay. 2019.

[42] Max-Philipp B. Schrader. gym-sokoban. https://github.com/mpSchrader/gym-sokoban, 2018.

[43] Florian Schroff, Dmitry Kalenichenko, and James Philbin. Facenet: A unified embedding for face recognition and clustering. In *Conference on Computer Vision and Pattern Recognition (CVPR)*, pages 815–823, 2015.

[44] John Schulman, Filip Wolski, Prafulla Dhariwal, Alec Radford, and Oleg Klimov. Proximal policy optimization algorithms. *CoRR*, abs/1707.06347, 2017.

[45] Nisan Stiennon, Long Ouyang, Jeffrey Wu, Daniel Ziegler, Ryan Lowe, Chelsea Voss, Alec Radford, Dario Amodei, and Paul F Christiano. Learning to summarize with human feedback. In *Advances in Neural Information Processing Systems (NeurIPS)*, volume 33, pages 3008–3021, 2020.

[46] Shan Suthaharan. Support vector machine. In *Machine learning models and algorithms for big data classification: thinking with examples for effective learning*, pages 207–235. Springer, 2016.

[47] Richard S Sutton, Andrew G Barto, et al. *Reinforcement learning: An introduction*, volume 1. MIT press Cambridge, 1998.

[48] Christian Szegedy, Vincent Vanhoucke, Sergey Ioffe, Jon Shlens, and Zbigniew Wojna. Rethinking the inception architecture for computer vision. In *IEEE/CVF conference on computer vision and pattern recognition (CVPR)*, pages 2818–2826, 2016.

[49] Csaba Szepesvári. Algorithms for reinforcement learning. *Synthesis lectures on artificial intelligence and machine learning*, 4(1):1–103, 2010.

[50] Yuval Tassa, Yotam Doron, Alistair Muldal, Tom Erez, Yazhe Li, Diego de Las Casas, David Budden, Abbas Abdolmaleki, Josh Merel, Andrew Lefrancq, et al. Deepmind control suite. *arXiv preprint arXiv:1801.00690*, 2018.

[51] Songjun Tu, Jingbo Sun, Qichao Zhang, Yaocheng Zhang, Jia Liu, Ke Chen, and Dongbin Zhao. In-dataset trajectory return regularization for offline preference-based reinforcement learning. In *AAAI Conference on Artificial Intelligence (AAAI)*, volume 39, pages 20929–20937, 2025.

[52] Saran Tunyasuvunakool, Alistair Muldal, Yotam Doron, Siqi Liu, Steven Bohez, Josh Merel, Tom Erez, Timothy Lillicrap, Nicolas Heess, and Yuval Tassa. dm_control: Software and tasks for continuous control. *Software Impacts*, 6:100022, 2020.

[53] Qing Wang, Jiechao Xiong, Lei Han, peng sun, Han Liu, and Tong Zhang. Exponentially weighted imitation learning for batched historical data. In *Advances in Neural Information Processing Systems (NeurIPS)*, volume 31, 2018.

[54] Songsheng Wang, Rucheng Yu, Zhihang Yuan, Chao Yu, Feng Gao, Yu Wang, and Derek F Wong. Spec-vla: speculative decoding for vision-language-action models with relaxed acceptance. *arXiv preprint arXiv:2507.22424*, 2025.

[55] Xiaofei Wang, Kimin Lee, Kourosh Hakhamaneshi, Pieter Abbeel, and Michael Laskin. Skill preferences: Learning to extract and execute robotic skills from human feedback. In *Conference on Robot Learning (CoRL)*, volume 164, pages 1259–1268, 08–11 Nov 2022.

[56] Xihuai Wang*, Shao Zhang*, Wenhao Zhang, Wentao Dong, Jingxiao Chen, Ying Wen, and Weinan Zhang. Zsc-eval: An evaluation toolkit and benchmark for multi-agent zero-shot coordination. *The 38th Conference on Neural Information Processing Systems (NeurIPS 2024) Track on Datasets and Benchmarks*, 2024.

[57] Yuanfei Wang, Fangwei Zhong, Jing Xu, and Yizhou Wang. Tom2c: Target-oriented multi-agent communication and cooperation with theory of mind. In *International Conference on Learning Representations (ICLR)*, 2022.

[58] Yuanfei Wang, Xiaojie Zhang, Ruihai Wu, Yu Li, Yan Shen, Mingdong Wu, Zhaofeng He, Yizhou Wang, and Hao Dong. Adamanip: Adaptive articulated object manipulation environments and policy learning. In *International Conference on Learning Representations (ICLR)*, 2025.

[59] Ali Yahya, Adrian Li, Mrinal Kalakrishnan, Yevgen Chebotar, and Sergey Levine. Collective robot reinforcement learning with distributed asynchronous guided policy search. In *International Conference on Intelligent Robots and Systems (IROS)*, pages 79–86, 2017.

[60] Zhenjie Yang, Xiaosong Jia, Hongyang Li, and Junchi Yan. Llm4drive: A survey of large language models for autonomous driving. *arXiv preprint arXiv:2311.01043*, 2023.

[61] Zhenjie Yang, Yilin Chai, Xiaosong Jia, Qifeng Li, Yuqian Shao, Xuekai Zhu, Haisheng Su, and Junchi Yan. Drivemoe: Mixture-of-experts for vision-language-action model in end-to-end autonomous driving. *arXiv preprint arXiv:2505.16278*, 2025.

[62] Zhenjie Yang, Xiaosong Jia, Qifeng Li, Xue Yang, Maoqing Yao, and Junchi Yan. Raw2drive: Reinforcement learning with aligned world models for end-to-end autonomous driving (in carla v2). *arXiv preprint arXiv:2505.16394*, 2025.

[63] Tianhe Yu, Deirdre Quillen, Zhanpeng He, Ryan Julian, Karol Hausman, Chelsea Finn, and Sergey Levine. Meta-world: A benchmark and evaluation for multi-task and meta reinforcement learning. In *Conference on Robot Learning (CoRL)*, volume 100, pages 1094–1100. PMLR, 2020.

[64] Hongming Zhang, Chenjun Xiao, Han Wang, Jun Jin, bo xu, and Martin Müller. Replay memory as an empirical MDP: Combining conservative estimation with experience replay. In *The Eleventh International Conference on Learning Representations (ICLR)*, 2023.

[65] Hongming Zhang, Tongzheng Ren, Chenjun Xiao, Dale Schuurmans, and Bo Dai. Provable representation with efficient planning for partially observable reinforcement learning. In *International Conference on Machine Learning (ICML)*, pages 59759–59782, 2024.

[66] Hongming Zhang, Ke Sun, bo xu, Linglong Kong, and Martin Müller. A distance-based anomaly detection framework for deep reinforcement learning. *Transactions on Machine Learning Research*, 2024. ISSN 2835-8856.

[67] Hongming Zhang, Chenjun Xiao, Chao Gao, Han Wang, Martin Müller, et al. Exploiting the replay memory before exploring the environment: enhancing reinforcement learning through empirical mdp iteration. *Advances in Neural Information Processing Systems (NeurIPS)*, 37: 85658–85692, 2024.

[68] Hongming Zhang, Fengshuo Bai, Chenjun Xiao, Chao Gao, Bo Xu, and Martin Müller. β-dqn: Improving deep q-learning by evolving the behavior. In *International Conference on Autonomous Agents and Multiagent Systems (AAMAS)*, pages 2317–2326, 2025.

[69] Ming Zhang, Shenghan Zhang, Zhenjie Yang, Lekai Chen, Jinliang Zheng, Chao Yang, Chuming Li, Hang Zhou, Yazhe Niu, and Yu Liu. Gobigger: A scalable platform for cooperative-competitive multi-agent interactive simulation. In *International Conference on Learning Representations (ICLR)*, 2023.

[70] Xiaojie Zhang, Yuanfei Wang, Ruihai Wu, Kunqi Xu, Yu Li, Liuyu Xiang, Hao Dong, and Zhaofeng He. Adaptive articulated object manipulation on the fly with foundation model reasoning and part grounding. *arXiv preprint arXiv:2507.18276*, 2025.

[71] Rui Zhao, Xu Liu, Yizheng Zhang, Minghao Li, Cheng Zhou, Shuai Li, and Lei Han. Craftenv: A flexible collective robotic construction environment for multi-agent reinforcement learning. In *International Conference on Autonomous Agents and Multiagent Systems (AAMAS)*, page 1164–1172, 2023.

[72] Guangxiang Zhu, Zichuan Lin, Guangwen Yang, and Chongjie Zhang. Episodic reinforcement learning with associative memory. In *International Conference on Learning Representations (ICLR)*, 2020.

[73] Xuekai Zhu, Daixuan Cheng, Dinghuai Zhang, Hengli Li, Kaiyan Zhang, Che Jiang, Youbang Sun, Ermo Hua, Yuxin Zuo, Xingtai Lv, et al. Flowrl: Matching reward distributions for llm reasoning. *arXiv preprint arXiv:2509.15207*, 2025.

[74] Yuke Zhu, Josiah Wong, Ajay Mandlekar, and Roberto Martín-Martín. robosuite: A modular simulation framework and benchmark for robot learning. *arXiv preprint arXiv:2009.12293*, 2020.

Supplementary Material

Table of Contents

A Full Procedure of STAR

A.1 Overview

Our method builds on the PbRL framework PEBBLE [24], which serves as a backbone for many online PbRL algorithms [37, 28]. In this paper, we propose a generic and flexible algorithm that can be seamlessly integrated with any PbRL algorithm and adapted to various settings, including discrete and continuous action spaces, as well as online and offline environments. The detailed procedures of our method are presented in Algorithm 1 for online settings and Algorithm 2 for offline settings.

For online settings, STAR introduces two distinct constrained operators for conservative Q-value estimation: $\max$ for discrete action spaces and $\mathcal{T}$ for continuous action spaces. These operators ensure more reliable policy learning by constraining overestimation in different action domains. In offline settings, our method first trains the reward model $\widehat{r}_\psi$ using pre-collected human preference data, then proceeds to policy learning, carefully addressing the challenges of limited feedback and bias inherent in offline RL.

Algorithm 1 STAR (Online)

```
Require: preference query frequency $K$, number of human's preference labels per session $M$
 1: Initialize parameters of $Q_\theta$, $\pi_\phi$, $\widehat{r}_\psi$, $Q_\xi$ and preference dataset $\mathcal{D} \leftarrow \emptyset$
 2: Initialize replay buffer $\mathcal{B}$ and $\pi_\theta$ with unsupervised exploration
 3: for each iteration do
 4:     Take action $a_t \sim \pi_\theta$ and collect $s_{t+1}$
 5:     if iteration $\% K == 0$ then
 6:         // Query preference
 7:         Sample pair of trajectories $(\sigma^0, \sigma^1)$ and query human for $y$
 8:         Store preference data into dataset $\mathcal{D} \leftarrow \mathcal{D} \cup \{(\sigma^0, \sigma^1, y)\}$
 9:         // Reward learning
10:         Sample batch $\{(\sigma^0, \sigma^1, y)_i\}_{i=1}^n$ from $\mathcal{D}$
11:         Optimize Equation (2) to update $\widehat{r}_\psi$
12:         Relabel the replay buffer $\mathcal{B}$ using $\widehat{r}_\psi$
13:     end if
14:     // Estimate conservative $\widehat{Q}$
15:     Store transition $(s_t, a_t, \widehat{r}_\psi(s_t, a_t), s_{t+1})$ into replay buffer $\mathcal{B}$
16:     Drive $\widehat{Q}$ via Equation (11) (discrete setting)
17:     Update $Q_\xi$ via Equation (9) (continuous setting)
18:     // Policy regularization
19:     Update $Q_\theta$ according to Equation (12).(discrete setting)
20:     Update $Q_\theta$ and $\pi_\phi$ according to Equation (4) and Equation (3), respectively.(continuous setting)
21: end for
Ensure: policy $\pi_\phi$
```

Algorithm 2 STAR (Offline)

```
Require: preference dataset $\mathcal{D}$, dataset $\mathcal{B}$
 1: Initialize parameters of $Q_\theta$, $\pi_\phi$, $\widehat{r}_\psi$
 2: // Reward learning
 3: Optimize Equation (2) to update $\widehat{r}_\psi$ with preference data from $\mathcal{D}$
 4: Label the dataset $\mathcal{B}$ via $\widehat{r}_\psi$
 5: for each iteration do
 6:     Sample a batch $(s, a, \widehat{r}_\psi(s, a), s')$ from $\mathcal{B}$
 7:     // Estimate conservative $\widehat{Q}$
 8:     Drive $\widehat{Q}$ via Equation (11) (discrete setting)
 9:     Update $Q_\xi$ via Equation (9) (continuous setting)
10:     // Policy regularization
11:     Update $Q_\theta$ according to Equation (12).(discrete setting)
12:     Update $Q_\theta$ and $\pi_\phi$ according to Equation (4) and Equation (3), respectively.(continuous setting)
13: end for
Ensure: policy $\pi_\phi$
```

A.2 Discrete Settings

In online settings with discrete action spaces, we provide an efficient implementation for bootstrapping a conservative estimate $\widehat{Q}$. By leveraging well-supported state-action pairs from the current replay memory, we generate conservative Q-value estimates that mitigate overestimation risks. Specifically, we structure the replay memory as a graph for discrete action spaces, following a similar approach to Zhu et al. [72], Hong et al. [15], Zhang et al. [64]. This graph-based structure allows us to efficiently perform conservative estimations by identifying connections between state-action pairs, enabling rapid updates without incurring significant computational overhead.

Conservative Estimate $\widehat{Q}$. We structure the replay memory as a dynamic and directed graph, denoted as $\mathcal{G} = (\mathcal{V}, \mathcal{E})$. Each vertex in this graph represents a state s paired with its associated action value estimation $\widehat{Q}(s, \cdot)$, forming the vertex set: $\mathcal{V} = \{s|(s, \widehat{Q}(s, \cdot))\}$. Each directed edge represents a transition from state s to state s' via action a, storing both the estimated reward $\widehat{r}_\psi(s, a)$ and the transition count $N(s, a, s')$. These elements are essential for updating the model based on experience. The edge set is represented as $\mathcal{E} = \{s \xrightarrow{a} s'|(a, \widehat{r}_\psi(s, a), N(s, a, s'), \widehat{Q}(s, a))\}$. To achieve efficient querying, each vertex and edge is assigned a unique key through a hash function, ensuring a query time complexity of $\mathcal{O}(1)$. This allows the graph to handle dynamic updates without significant overhead. Each vertex v contains an action set $\partial\mathcal{A}(s)$, which tracks the actions executed in state s, facilitating in-sample updates and improving learning efficiency. Similar to conventional replay memory, this graph stores the most recent experiences while maintaining a fixed memory size to prevent excessive memory usage.

This graph updating contains two primary components: estimation updating and reward relabeling. When a new transition $(s, a, \widehat{r}_\psi(s, a), s')$ is observed, a new vertex and edge are added to the graph based on the previously outlined structure, initializing $\widehat{Q}(s, a) = 0$ and setting $N(s, a, s') = 1$. If the edge for the transition already exists, the visit count is incremented: $N(s, a, s') \leftarrow N(s, a, s') + 1$, allowing the graph to adapt to repeated experiences and refine its estimation over time.

For updating the action value estimate $\widehat{Q}$, we sample a subset of graph vertices $\partial\mathcal{V} \subseteq \mathcal{V}$ in reverse order, similar to the techniques used by Rotinov [41], Lee et al. [25]. This reverse-order sampling improves the efficiency of the updates by leveraging the structure of the graph, allowing for rapid convergence of $\widehat{Q}$. During this process, the max-operator is constrained to operate over the in-sample action set $\partial\mathcal{A}(s)$ rather than the entire action space. This ensures that the method remains focused on well-explored actions, reducing the risk of overestimation by avoiding out-of-sample actions.

The value iteration process is defined as:

$$\widehat{Q}(s, a) \leftarrow \sum_{s' \in \mathcal{S}} \widehat{p}(s'|s, a)\Big[\widehat{r}_\psi(s, a) + \gamma \max_{a' \in \partial\mathcal{A}(s')} \widehat{Q}(s', a')\Big], \tag{11}$$

where the empirical transition dynamics $\widehat{p}(s'|s, a) = N(s, a, s')/\sum_{s'} N(s, a, s')$ are computed from the graph. This update rule ensures that unseen actions are not queried during value estimation, thereby preventing overestimation.

For reward relabeling, each time the reward model $\widehat{r}_\psi$ is updated, all past experiences in the graph are relabeled according to the updated model. This maximizes the utility of historical data and accounts for non-stationary reward functions. While this relabeling process can be computationally intensive as the number of stored transitions grows, it allows the algorithm to adapt to changing reward landscapes and ensures that the learning process remains up-to-date with the most accurate reward information.

Updating Q_θ. In scenarios with discrete actions, we define $\widehat{\pi}$ as the Boltzmann policy derived from $\widehat{Q}$, where $\widehat{\pi}(s) = \text{Softmax}_{a \in \partial\mathcal{A}(s)}(\widehat{Q}(s, \cdot))$. This policy is inherently conservative, considering only the support set $\partial\mathcal{A}(s)$ for a given state s. Similarly, the policy π, derived from the Q_θ network, is expressed as $\pi(s) = \text{Softmax}_{a \in \partial\mathcal{A}(s)}(Q_\theta(s, \cdot))$. Total loss is defined as follows:

$$\mathcal{L}_{\text{discrete}}(\theta) = \mathop{\mathbb{E}}_{\tau_t \sim \mathcal{G}}\Big[(Q_\theta(s, a) - y)^2\Big] + \eta\mathcal{L}_{\text{reg}}(\theta), \tag{12}$$

where $y = \widehat{r}_\psi(s, a) + \gamma \max_{a'} Q(s', a')$ is the Q target, $\tau_t = (s_t, a_t, s_{t+1}, \widehat{r}_\psi(s_t, a_t))$ is the transition and η is the weight factor.

B Theoretical Analysis

B.1 Reward Overfitting Analysis

Why Reward Overfitting? For reward learning, the logits output by the reward model are transformed into probabilities using a softmax function, ensuring that the resulting probabilities sum to 1. The loss function in equation (13) is used to optimize r_ψ as follows:

$$\mathcal{L}_{\text{reward}}(\psi) = - \mathop{\mathbb{E}}_{(\sigma^0,\sigma^1,y)\sim\mathcal{D}} \Big[y(0) \log P_\psi[\sigma^0 \succ \sigma^1] + y(1) \log P_\psi[\sigma^1 \succ \sigma^0] \Big]. \tag{13}$$

In the optimal scenario, we aim for the predicted probability of the preferred segment to be 1, while the rejected segment's predicted probability should be 0. This can be represented mathematically as:

$$\begin{aligned} \frac{\exp(\sum_t \widehat{r}_\psi(s_t^0, a_t^0))}{\exp(\sum_t \widehat{r}_\psi(s_t^0, a_t^0)) + \exp(\sum_t \widehat{r}_\psi(s_t^1, a_t^1))} &= 1 \\ \frac{\exp(\sum_t \widehat{r}_\psi(s_t^1, a_t^1))}{\exp(\sum_t \widehat{r}_\psi(s_t^0, a_t^0)) + \exp(\sum_t \widehat{r}_\psi(s_t^1, a_t^1))} &= 0 \end{aligned} \tag{14}$$

Expanding the softmax expressions in equation (14) yields the following analytical solution:

$$\begin{aligned} &\exp(\sum_t \widehat{r}_\psi(s_t^0, a_t^0)) = \exp(\sum_t \widehat{r}_\psi(s_t^0, a_t^0)) + \exp(\sum_t \widehat{r}_\psi(s_t^1, a_t^1)) \\ &\quad \sum_t \widehat{r}_\psi(s_t^0, a_t^0) = \log\left(\exp(\sum_t \widehat{r}_\psi(s_t^0, a_t^0)) + \exp(\sum_t \widehat{r}_\psi(s_t^1, a_t^1)) \right) \\ &\exp(\sum_t \widehat{r}_\psi(s_t^1, a_t^1)) = 0 \\ &\quad \sum_t \widehat{r}_\psi(s_t^1, a_t^1) = -\infty \end{aligned} \tag{15}$$

Upon examining this analytical solution in equation (15), we observe that for the reward model to predict optimal behavior, the preferred segments must be assigned a constant value, while the rejected segments approach negative infinity. However, achieving this theoretical optimal solution is practically impossible, as it would lead to overfitting. In practice, this results in the reward model being overly confident in its predictions, causing poor generalization to new data.

Why preference margin regularization effect? To address this issue, we introduce a margin technique inspired by Szegedy et al. [48]. By introducing a bounded objective in reward optimization, we constrain the reward model, preventing it from overoptimizing the loss function and ensuring that the analytical solution remains bounded. The specific update rule is as follows:

$$y(i,j) = \begin{cases} (1-\varepsilon, \varepsilon), & \text{if } \sigma^i \succ \sigma^j \\ (0.5, 0.5), & \text{otherwise.} \end{cases} \tag{16}$$

where ε is margin factor.

Under preference margin regularization, we aim for the predicted probability of the preferred segment to be $1-\varepsilon$, while the rejected segment's predicted probability should be ε. This can be represented mathematically as:

$$\begin{aligned} \frac{\exp(\sum_t \widehat{r}_\psi(s_t^0, a_t^0))}{\exp(\sum_t \widehat{r}_\psi(s_t^0, a_t^0)) + \exp(\sum_t \widehat{r}_\psi(s_t^1, a_t^1))} &= 1-\varepsilon \\ \frac{\exp(\sum_t \widehat{r}_\psi(s_t^0, a_t^1))}{\exp(\sum_t \widehat{r}_\psi(s_t^0, a_t^0)) + \exp(\sum_t \widehat{r}_\psi(s_t^1, a_t^1))} &= \varepsilon \end{aligned} \tag{17}$$

Expanding the softmax expressions in equation (17) yields the following analytical solution:

$$
\begin{aligned}
\exp(\sum_t \widehat{r}_\psi(s_t^0, a_t^0)) &= (1-\varepsilon) * \exp(\sum_t \widehat{r}_\psi(s_t^0, a_t^0)) + (1-\varepsilon) * \exp(\sum_t \widehat{r}_\psi(s_t^1, a_t^1)) \\
\varepsilon * \exp(\sum_t \widehat{r}_\psi(s_t^0, a_t^0)) &= (1-\varepsilon) * \exp(\sum_t \widehat{r}_\psi(s_t^1, a_t^1)) \\
\sum_t \widehat{r}_\psi(s_t^0, a_t^0) - \sum_t \widehat{r}_\psi(s_t^1, a_t^1) &= \log\left(\frac{1-\varepsilon}{\varepsilon}\right)
\end{aligned}
\tag{18}
$$

From the derivation in equation (18), we observe that after applying preference margin regularization, the objective shifts from maximizing the difference between preferred and rejected samples to maintaining a controlled margin. Specifically, preference margin regularization introduces a bounded margin of $\log\left(\frac{1-\varepsilon}{\varepsilon}\right)$ between positive and negative samples. This ensures that we do not overly optimize the loss during reward learning, which could lead to overfitting.

The key insight behind preference margin regularization is that it limits the optimization process, preventing the model from becoming overly confident in its predictions by capping the margin between preferred and rejected samples. By keeping the margin bounded, preference margin regularization helps stabilize the learning process, reducing the risk of overfitting and improving the model's ability to generalize to unseen states.

B.2 Proof of Theorem 4.1

In this section, we analyze the property of $\widehat{Q}$ in finite state-action space $\mathcal{S} \times \mathcal{A}$. The proof of $\lim_{t\to\infty} Q_t = Q^*$ has been well-established in previous work [40, 18, 31]. Then the proof of $\lim_{t\to\infty} \widehat{Q}_t = \widehat{Q}^*$ is similar. We first prove the empirical Bellman operator Equation (21) is a γ-contraction operator under the supremum norm. Then when updating in a sampling manner as Equation (22), it can be considered as a random process. Borrowing an auxiliary result from stochastic approximation, we prove it satisfies the conditions that guarantee convergence. Finally, to prove $\widehat{Q}^*$ lower-bounds Q^*, we rewrite $\widehat{Q}^*(s,a) - Q^*(s,a)$ based on the standard and empirical Bellman operators. When the data covers the whole state-action space, we naturally have $\widehat{Q}^* = Q^*$.

For proof simplicity, we use β denotes policies that interact with the environment and form the current replay memory. We first show existing results for Bellman learning in Equation (20), and then prove Theorem 4.1 in three steps. The Bellman (optimality) operator $\mathcal{B}$ is defined as:

$$
(\mathcal{B}Q)(s,a) = \sum_{s'\in\mathcal{S}} P(s'|s,a)[r + \gamma \max_{a'} Q(s',a')]. \tag{19}
$$

Previous works have shown the operator $\mathcal{B}$ is a γ-contraction with respect to supremum norm:

$$
\|\mathcal{B}Q_1 - \mathcal{B}Q_2\|_\infty \leq \gamma \|Q_1 - Q_2\|_\infty,
$$

the supremum norm $\|v\|_\infty = \max_{1\leq i\leq d} |v_i|$, d is the dimension of vector v. Following Banach's fixed-point theorem, Q converges to optimal action value Q^* if we consecutively apply operator $\mathcal{B}$ to Q, $\lim_{n\to\infty} (\mathcal{B})^n Q = Q^*$.

Further, the update rule in Equation (20), i.e. Q-learning, is a sampling version that applies the γ-contraction operator $\mathcal{B}$ to Q.

$$
Q(s,a) \leftarrow r(s,a) + \gamma \max_{a'} Q(s',a'). \tag{20}
$$

It can be considered as a random process and will converge to Q^*, $\lim_{t\to\infty} Q_t = Q^*$, with some mild conditions [49, 40, 18, 31].

Similarly, we define the empirical Bellman (optimality) operator $\hat{\mathcal{B}}$ as:

$$
(\hat{\mathcal{B}}\widehat{Q})(s,a) = \sum_{s'\in\mathcal{S}} P(s'|s,a)[r + \gamma \max_{a':\beta(a'|s')>0} \widehat{Q}(s',a')]. \tag{21}
$$

And the sampling version is:

$$
\widehat{Q}(s,a) \leftarrow r + \gamma \max_{a':\beta(a'|s')>0} \widehat{Q}(s',a'), \tag{22}
$$

We split Theorem 4.1 into three lemmas. We first show $\hat{\mathcal{B}}$ is a γ-contraction operator under supremum norm, thus converges to optimal action value $\widehat{Q}^*$, $\lim_{n\to\infty}(\mathcal{B})^n\widehat{Q} = \widehat{Q}^*$. Then we show the sampling-based update rule in Equation (22) converges to $\widehat{Q}^*$, $\lim_{t\to\infty}\widehat{Q}_t = \widehat{Q}^*$. Finally, we show $\widehat{Q}^*$ lower-bounds Q^*, $\widehat{Q}^*(s,a) - Q^*(s,a) \leq 0, \forall(s,a) \in \mathcal{S}\times\mathcal{A}$. And when the data covers the whole state-action space, i.e. $\beta(a|s) > 0$ for all state-action pairs, we naturally have $\widehat{Q}^*(s,a) = Q^*(s,a)$.

Lemma B.1. *The operator $\hat{\mathcal{B}}$ defined in Equation (21) is a γ-contraction operator under supremum norm,*

$$\|\hat{\mathcal{B}}\widehat{Q}_1 - \hat{\mathcal{B}}\widehat{Q}_2\|_\infty \leq \gamma\|\widehat{Q}_1 - \widehat{Q}_2\|_\infty.$$

Proof. We can rewrite $\|\hat{\mathcal{B}}\widehat{Q}_1 - \hat{\mathcal{B}}\widehat{Q}_2\|_\infty$ as

$$\begin{aligned}
&\|\hat{\mathcal{B}}\widehat{Q}_1 - \hat{\mathcal{B}}\widehat{Q}_2\|_\infty \\
&= \max_{s,a}\Big|\sum_{s'\in\mathcal{S}} P(s'|s,a)[r + \gamma \max_{a_1':\beta(a_1'|s')>0}\widehat{Q}_1(s',a_1')] - P(s'|s,a)[r + \gamma\max_{a_2':\beta(a_2'|s')>0}\widehat{Q}_2(s',a_2')]\Big| \\
&= \max_{s,a}\gamma\Big|\sum_{s'\in\mathcal{S}} P(s'|s,a)[\max_{a_1':\beta(a_1'|s')>0}\widehat{Q}_1(s',a_1') - \max_{a_2':\beta(a_2'|s')>0}\widehat{Q}_2(s',a_2')]\Big| \\
&\leq \max_{s,a}\gamma\sum_{s'\in\mathcal{S}} P(s'|s,a)\Big|\max_{a_1':\beta(a_1'|s')>0}\widehat{Q}_1(s',a_1') - \max_{a_2':\beta(a_2'|s')>0}\widehat{Q}_2(s',a_2')\Big| \\
&\leq \max_{s,a}\gamma\sum_{s'\in\mathcal{S}} P(s'|s,a)\max_{\tilde{a}:\beta(\tilde{a}|s')>0}\Big|\widehat{Q}_1(s',\tilde{a}) - \widehat{Q}_2(s',\tilde{a})\Big| \\
&\leq \max_{s,a}\gamma\sum_{s'\in\mathcal{S}} P(s'|s,a)\max_{\tilde{s},\tilde{a}:\beta(\tilde{a}|\tilde{s})>0}\Big|\widehat{Q}_1(\tilde{s},\tilde{a}) - \widehat{Q}_2(\tilde{s},\tilde{a})\Big| \\
&= \max_{s,a}\gamma\sum_{s'\in\mathcal{S}} P(s'|s,a)\|\widehat{Q}_1 - \widehat{Q}_2\|_\infty \\
&= \gamma\|\widehat{Q}_1 - \widehat{Q}_2\|_\infty,
\end{aligned}$$

where the last line follows from $\sum_{s'\in\mathcal{S}} P(s'|s,a) = 1$. ☐

To show the sampling-based update rule in Equation (22) converges to $\widehat{Q}^*$, we borrow an auxiliary result from stochastic approximation [40, 18].

Theorem B.2. *The random process $\{\Delta_t\}$ taking values in $\mathbb{R}^n$ and defined as*

$$\Delta_{t+1}(x) = (1 - \alpha_t(x))\Delta_t(x) + \alpha_t(x)F_t(x) \tag{23}$$

converges to zero w.p.1 under the following assumptions:

(1) $0 \leq \alpha_t \leq 1, \sum_t \alpha_t(x) = \infty$ *and* $\sum_t \alpha_t^2(x) < \infty$*;*

(2) $\|\mathbb{E}[F_t(x)|\mathcal{F}_t]\|_W \leq \gamma\|\Delta_t\|_W$*, with* $\gamma < 1$*;*

(3) $Var[F_t(x)|\mathcal{F}_t] \leq C(1 + \|\Delta_t\|_W^2)$*, for* $C > 0$.

W is a norm. In our proof it is a supremum norm.

Proof. See Robbins and Monro [40], Jaakkola et al. [18]. ☐

Lemma B.3. *Given any initial estimation $\widehat{Q}_0$, the following update rule:*

$$\widehat{Q}_{t+1}(s_t,a_t) = \widehat{Q}_t(s_t,a_t) + \alpha_t(x_t,a_t)[r_t + \gamma\max_{a:\beta(a|s_{t+1})>0}\widehat{Q}_t(s_{t+1},a) - \widehat{Q}_t(s_t,a_t)], \tag{24}$$

converges w.p.1 to the optimal action-value function $\widehat{Q}^*$ if

$$0 \leq \alpha_t(s,a) \leq 1, \quad \sum_t \alpha_t(s,a) = \infty \quad \textit{and} \quad \sum_t \alpha_t^2(s,a) < \infty,$$

for all $(s,a) \in \mathcal{S}\times\mathcal{A}$.

Proof. Based on Theorem B.2, we prove the update rule in Equation (24) converges.

Rewrite Equation (24) as

$$\widehat{Q}_{t+1}(s_t, a_t) = (1 - \alpha_t(s_t, a_t))\widehat{Q}_t(s_t, a_t) + \alpha_t(x_t, a_t)[r_t + \gamma \max_{a:\beta(a|s_{t+1})>0} \widehat{Q}_t(s_{t+1}, a)]$$

Subtract $\widehat{Q}^*(s_t, a_t)$ from both sides:

$$\begin{aligned}&\widehat{Q}_{t+1}(s_t, a_t) - \widehat{Q}^*(s_t, a_t)\\ =\ &(1 - \alpha_t(s_t, a_t))(\widehat{Q}_t(s_t, a_t) - \widehat{Q}^*(s_t, a_t)) + \alpha_t(x_t, a_t)[r_t + \gamma \max_{a:\beta(a|s_{t+1})>0} \widehat{Q}_t(s_{t+1}, a) - \widehat{Q}^*(s_t, a_t)]\end{aligned}$$

Let

$$\Delta_t(s, a) = \widehat{Q}(s, a) - \widehat{Q}^*(s, a) \tag{25}$$

and

$$F_t(s, a) = r + \gamma \max_{a':\beta(a'|s')>0} \widehat{Q}_t(s', a') - \widehat{Q}^*(s, a). \tag{26}$$

We get the same random process shown in Theorem B.2 Equation (23). Then, proving $\lim_{t\to\infty} \widehat{Q}_t = \widehat{Q}^*$ is the same as proving $\Delta_t(s, a)$ converges to zero with probability 1. We only need to show the assumptions in Theorem B.2 are satisfied under the definitions of Equations (25) and (26).

Theorem B.2 (1) is the same as the condition in Lemma B.3. It is easy to achieve, for example, we can choose $\alpha_t(s, a) = 1/t$.

For Theorem B.2 (2), we have

$$\begin{aligned}\mathbb{E}[F_t(s, a)|\mathcal{F}_t] &= \sum_{s'\in\mathcal{S}} P(s'|s, a)[r + \gamma \max_{a':\beta(a'|s')} \widehat{Q}_t(s', a') - \widehat{Q}^*(s, a)]\\ &= (\hat{\mathcal{B}}\widehat{Q}_t)(s, a) - \widehat{Q}^*(s, a)\\ &= (\hat{\mathcal{B}}\widehat{Q}_t)(s, a) - (\hat{\mathcal{B}}\widehat{Q}^*)(s, a)\end{aligned}$$

Thus,

$$\begin{aligned}\|\mathbb{E}[F_t(s, a)|\mathcal{F}_t]\|_\infty &= \|(\hat{\mathcal{B}}\widehat{Q}_t) - (\hat{\mathcal{B}}\widehat{Q}^*)\|_\infty\\ &\le \gamma\|\widehat{Q}_t - \widehat{Q}^*\|_\infty\\ &= \gamma\|\Delta_t\|_\infty,\end{aligned}$$

with $\gamma < 1$.

For Theorem B.2 (3), we have

$$\begin{aligned}Var[F_t(s)|\mathcal{F}_t] &= \mathbb{E}[F_t(s) - \mathbb{E}[F_t(s)|\mathcal{F}_t]|\mathcal{F}_t]^2\\ &= \mathbb{E}[F_t(s) - ((\hat{\mathcal{B}}\widehat{Q}_t)(s, a) - (\hat{\mathcal{B}}\widehat{Q}^*)(s, a))]^2\\ &= \mathbb{E}[r + \gamma \max_{a':\beta(a'|s')>0} \widehat{Q}_t(s', a') - \widehat{Q}^*(s, a) - ((\hat{\mathcal{B}}\widehat{Q}_t)(s, a) - (\hat{\mathcal{B}}\widehat{Q}^*)(s, a))]^2\\ &= \mathbb{E}[r + \gamma \max_{a':\beta(a'|s')>0} \widehat{Q}_t(s', a') - (\hat{\mathcal{B}}\widehat{Q}_t)(s, a)]^2\\ &= Var[r + \gamma \max_{a':\beta(a'|s')>0} \widehat{Q}_t(s', a')|\mathcal{F}_t]\end{aligned}$$

We add and minus a $\widehat{Q}^*$ term to make it close to the RHS in Theorem B.2 (3):

$$Var[r + \gamma \max_{a':\beta(a'|s')>0} \widehat{Q}^*(s', a') + \gamma \max_{a':\beta(a'|s')>0} \widehat{Q}_t(s', a') - \gamma \max_{a':\beta(a'|s')>0} \widehat{Q}^*(s', a')|\mathcal{F}_t]$$

Since r is bounded, thus $r + \gamma \max_{a':\beta(a'|s')>0} \widehat{Q}^*(s', a')$ is bounded. And clearly the second part $\max_{a':\beta(a'|s')>0} \widehat{Q}_t(s', a') - \max_{a':\beta(a'|s')>0} \widehat{Q}^*(s', a')$ can be bounded by $\|\Delta_t\|_\infty$ with some constant. Thus, we have

$$Var[F_t(s)|\mathcal{F}_t] \le C(1 + \|\Delta_t\|^2_\infty),$$

for some constant $C > 0$ under supremum norm. Thus, by Theorem B.2, Δ_t converges to zero w.p.1, i.e., $\widehat{Q}_t$ converges to $\widehat{Q}^*$ w.p.1. □

Lemma B.4. *The value estimation obtained by Equation* (21) *lower-bounds the value estimation obtained by Equation* (19)*:*

$$\widehat{Q}^*(s,a) - Q^*(s,a) \leq 0 \tag{27}$$

for all state-action pairs.

Proof. Following the definition of Equations (19) and (21), we can rewrite as

$$\begin{aligned}
&\max_{s,a}(\widehat{Q}^*(s,a) - Q^*(s,a)) \\
&= \max_{s,a}(\hat{\mathcal{B}}\widehat{Q}^*(s,a) - \mathcal{B}Q^*(s,a)) \\
&= \max_{s,a}\Big(\sum_{s'\in\mathcal{S}} P(s'|s,a)[r + \gamma \max_{\hat{a}':\beta(\hat{a}'|s')>0} \widehat{Q}^*(s',\hat{a}')] - \sum_{s'\in\mathcal{S}} P(s'|s,a)[r + \gamma \max_{a'} Q^*(s',a')]\Big) \\
&= \max_{s,a} \sum_{s'\in\mathcal{S}} P(s'|s,a)\gamma\big(\max_{\hat{a}':\beta(\hat{a}'|s')>0} \widehat{Q}^*(s',\hat{a}') - \max_{a'} Q^*(s',a')\big) \\
&\leq \max_{s,a} \sum_{s'\in\mathcal{S}} P(s'|s,a)\gamma\big(\max_{\hat{a}'} \widehat{Q}^*(s',\hat{a}') - \max_{a'} Q^*(s',a')\big) \\
&\leq \max_{s,a} \sum_{s'\in\mathcal{S}} P(s'|s,a)\gamma \max_{\tilde{a}}(\widehat{Q}^*(s',\tilde{a}) - Q^*(s',\tilde{a})) \\
&\leq \max_{s,a} \gamma \sum_{s'\in\mathcal{S}} P(s'|s,a) \max_{\tilde{s},\tilde{a}}(\widehat{Q}^*(\tilde{s},\tilde{a}) - Q^*(\tilde{s},\tilde{a})) \\
&= \gamma \max_{\tilde{s},\tilde{a}}(\widehat{Q}^*(\tilde{s},\tilde{a}) - Q^*(\tilde{s},\tilde{a})) = \gamma \max_{s,a}(\widehat{Q}^*(s,a) - Q^*(s,a))
\end{aligned}$$

where the last line follows from $\sum_{s'\in\mathcal{S}} P(s'|s,a) = 1$. Then we have

$$\begin{aligned}
\max_{s,a}(\widehat{Q}^*(s,a) - Q^*(s,a)) &\leq \gamma \max_{s,a}(\widehat{Q}^*(s,a) - Q^*(s,a)) \\
&\leq \gamma^2 \max_{s,a}(\widehat{Q}^*(s,a) - Q^*(s,a)) \\
&\leq \cdots \\
&\leq \gamma^n \max_{s,a}(\widehat{Q}^*(s,a) - Q^*(s,a))
\end{aligned}$$

Take limit for both sides and since $0 < \gamma < 1$, we have $\max_{s,a}(\widehat{Q}^*(s,a) - Q^*(s,a)) \leq 0$.

When $\beta(a|s) > 0$ for all state-action pairs, the two contraction operators $\hat{\mathcal{B}}$ and $\mathcal{B}$ are the same. And based on Banach's fixed-point theorem, there is a unique fixed point. Thus $\widehat{Q}^*(s,a) = Q^*(s,a)$ for all state-action pairs., i.e., $\widehat{Q}^*(s,a) - Q^*(s,a) = 0, (s,a) \in \mathcal{S} \times \mathcal{A}$ holds when $\beta(a|s) > 0$ for all state-action pairs. □

Then, we get Theorem 4.1 proved with Lemmas B.1, B.3 and B.4.

C Experimental Details

In this section, we outline the detailed implementation settings, including basic PbRL configurations, feedback setup in experiments, and other training details.

C.1 Preference-based RL Basic Settings

In this section, we provide additional details on unsupervised exploration and the uncertainty-based sampling scheme, as mentioned in Section 5.1. These techniques are crucial for improving feedback efficiency in algorithms, as referenced in Lee et al. [24]. To ensure a fair comparison, all preference-based RL algorithms in our experiments incorporate both unsupervised exploration and uncertainty-based sampling.

Unsupervised Exploration. Unsupervised exploration in preference-based RL, introduced by Lee et al. [24], involves designing an intrinsic reward based on the entropy of the state, effectively encouraging the agent to explore diverse states and generate varied behaviors. Specifically, it utilizes a variant of particle-based entropy [32] as a computationally convenient entropy estimation method.

Uncertainty-based Sampling. Several sampling schemes exist, including uniform sampling, disagreement sampling, and entropy sampling. The latter two are categorized as uncertainty-based sampling and have demonstrated superior performance compared to uniform sampling, both intuitively and empirically. In our experiments, all methods (in the online settings) employ disagreement sampling schemes.

C.2 Feedback in Experiments

Number of Feedback. In the **online setting**, we use 100 preference pairs for Cheetah Run, Button Press, and Window Open; 200 pairs for Walker Walk; 300 pairs for Push-5×5-1, Push-6×6-1, and Push-7×7-1; 1000 pairs for Quadruped Walk, Push-5×5-2, Push-6×6-2, Push-7×7-2, Strip-shaped Building, Block-shaped Building, and Simple Two-Story Building; and 4000 pairs for Sweep Into.

In the **offline setting**, we use 100 preference pairs for antmaze-medium-play-v2, antmaze-medium-diverse-v2, hopper-medium-expert-v2, walker2d-medium-expert-v2, can-ph, and lift-ph; 500 pairs for hopper-medium-replay-v2, walker2d-medium-replay-v2, can-mh, and lift-mh; and 1000 pairs for antmaze-large-play-v2 and antmaze-large-diverse-v2.

Human Labels. We incorporate human feedback from subjects with prior experience in robotic tasks, as outlined in PT [21][*]. An informed human annotator evaluates each task by watching video clips of trajectory segments and selecting the one that more effectively achieves the task objective. Each segment lasts 3 seconds (equivalent to 100 time steps). If no clear preference is observed, the annotator may assign equal preference to both segments by selecting a neutral option.

C.3 Architecture and hyperparameters.

In this section, we describe the architecture of the neural networks used in the SAC algorithm, which serves as the baseline method. The actor in SAC consists of two layers with 1024 hidden units. The two Q networks in SAC share the same architecture as the actor. This consistent architecture helps streamline the optimization process across the actor and critic networks. The detailed neural network parameters and hyperparameters for SAC are shown in Table 8a. Additionally, Table 8b presents the distinct hyperparameters for PEBBLE and STAR.

Hyperparameter	Value	Hyperparameter	Value
Discount	0.99	Batch size	1024
(β_1, β_2)	(0.9,0.999)	Initial temperature	0.1
Hidden layer units	1024	Critic target update freq	2
Activation Function	ReLU	Critic τ	0.005
Critic optimizer	AdamW	Learning rate	5e-4
Actor optimizer	AdamW		

(a) Hyperparameters of SAC.

Hyperparameter	Value	Hyperparameter	Value
Length of segment	50	Reward model size	3
Learning rate	0.0003	Frequency of feedback	5000
Reward batch size	128	Number of train steps	1e6
Reward update	200	Replay buffer capacity	1e6
Scaling parameter β (STAR)	6	Graph update batch size (STAR)	32
margin parameter ε (STAR)	0.05	Regularizer weight η (STAR)	0.1

(b) Hyperparameters of PEBBLE and STAR.

D Environment Specifications

In this section, we delineate the tasks utilized in our experiments. For online settings, discrete tasks include Sokoban [42] and Craftenv [71], while continuous tasks encompass robotic manip-

[*]https://github.com/csmile-1006/PreferenceTransformer

ulation challenges from Meta-world [63] and locomotion tasks from the DeepMind Control Suite (DMControl) [50, 52]. Regarding offline settings, we incorporate control tasks from the D4RL benchmarks [7].

D.1 Sokoban

Sokoban [42], the Japanese word for 'a warehouse keeper', is a puzzle video game, which is analogous to the problem of having an agent in a warehouse push some specified boxes from their initial locations to target locations. Target locations have the same number of boxes. The goal of the game is to manipulate the agent to move all boxes to the target locations. Specifically, the game is played on a rectangular grid called a room, and each cell of the room is either a floor or a wall. At each new episode, the environment will be reset, which means the layout of the room is randomly generated, including the floors, the walls, the target locations, the boxes' initial locations, and the location of the agent. We choose six tasks with different complexities from Push-5×5-1 to Push-7×7-2, which is shown in Figure 8. The numbers in the task name denote respectively the size of the grid and the number of boxes.

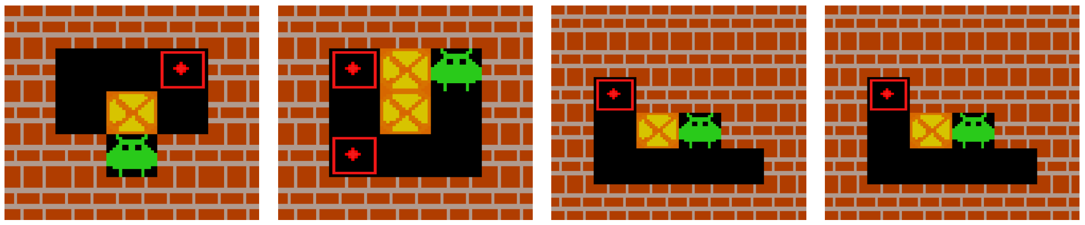

(a) Push-5x5-1 (b) Push-5x5-2 (c) Push-6x6-1 (d) Push-6x6-2

Figure 8: Visualization of puzzle tasks from Sokoban, which focuses on evaluating the capabilities of agents in spatial reasoning, logical deduction, and long-term planning.

State Space. The state space consists of all possible images displayed on the screen. Each image has the same size as the map, and using the way of dividing each pixel of the image by 255 to normalize into [0,1], we preprocess the image before inputting.

Action Space. The action space of Sokoban has a total of eight actions, composed of moving and pushing the box in four directions, which are *left*, *right*, *up*, *down*, *push-left*, *push-right*, *push-up*, *push-down* in detail.

Reward Setting. The agent gets a punishment with a -0.1 reward after each time step. Successfully pushing a box to the target location, can get a +1 reward, and if all boxes are laid in the right locations, the agent can obtain an extra +10 reward. We set the max episode steps to 120, which means the cumulative reward during one episode ranges from -12 to 10 plus the number of boxes.

D.2 CraftEnv

Craftenv [71], A Flexible Robotic Construction Environment, is a collection of construction tasks. The agent needs to learn to manipulate the elements, including smartcar, blocks, and slopes, to achieve a target structure through efficient and effective policy. Each construction task is a simulation of the corresponding complex real-world task, which is challenging enough for reinforcement learning algorithms. Meanwhile, the CraftEnv is highly malleable, enabling researchers to design their own tasks for specific requirements. The environment is simple to use since it is implemented by Python and can be rendered using PyBullet. We choose three different designs of the building tasks, shown in Figure 9, to evaluate our algorithm in CraftEnv.

State Space. We assume that the agent can obtain all the information in the map. Therefore, the state consists of all knowledge of smartcar, blocks, folded slopes, unfolded slopes' body, and unfolded slopes' foot, including the position and the yaw angle.

Action Space. The available actions of an agent are designed based on real-world smartcar models, including a total of fifteen actions. Besides all eight directions moving actions, i.e. *forward*, *backward*, *left*, *right*, *left-forward*, *left-backward*, *right-forward*, and *right-backward*, there are interaction-related actions, designed to simulate the building process in the real world. Specifically, the agent can act *lift*

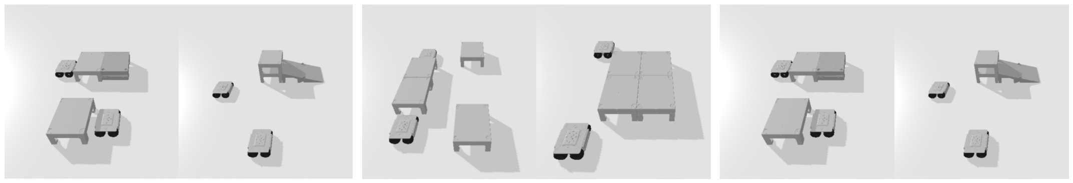

(a) The Strip-shaped Building (b) The Block-shaped Building (c) The Simple Two-Story Building

Figure 9: Visualization of building tasks from CraftEnv. From left to right are The Strip-shaped Building, The Block-shaped Building, and The Simple Two-Story Building task respectively.

and *drop* actions to decide whether or not to carry the surrounding basic element, and can *flod* or *unflod* slopes to build the complex buildings. In addition, the actions of *rotate-left* and *rotate-right* control the agent to rotate the main body to the left and right, and *stop* action is just a non-action.

Reward Setting. CraftEnv is a flexible environment as mentioned above. We can specify our own reward function for different construction tasks. For the relatively simple tasks of building with specified shape requirements, we can use discrete reward, where some reward is given when part of the blueprint is built. While, for building tasks with high complexity, various reward patterns should be designed to encourage the agent to build with different intentions.

D.3 Robotic tasks

In our experiments, we utilize robotic manipulation tasks from Meta-world [63] and locomotion tasks from the DeepMind Control Suite (DMControl) [50, 52], which is visualized in Figure 10. Meta-World comprises 50 diverse manipulation tasks with a common structural framework, while DMControl offers a collection of stable, rigorously tested tasks, serving as benchmarks for continuous control learning agents. These tasks are equipped with well-formulated reward functions that facilitate agent learning. For performance evaluation, Meta-world introduces an interpretable success metric for each task, which serves as the standard evaluation criterion across various settings. This metric often hinges on the proximity of task-relevant objects to their final goal positions, quantified as $||o - g|| \leq \epsilon$, with ϵ representing a nominal distance threshold, such as 5 cm. DMControl, conversely, employs episode returns for evaluation. We adopt fixed-length episodes of 1000 timesteps as a proxy. Given that all reward functions are designed such that $r \approx 1$ is in proximity to goal states, learning curves that measure total returns can maintain consistent y-axis limits of $[0, 1000]$. This uniformity simplifies interpretation and facilitates averaging across tasks.

D.4 D4RL benchmark

AntMaze. AntMaze involves a navigation challenge where a Mujoco Ant robot must locate and reach a specified goal. The data for this task is derived from a pre-trained policy designed to navigate various maze layouts, primarily focusing on two configurations: *medium* and *large*. The data are compiled using two distinct strategies: *diverse* and *play*. *Diverse* data sets are produced by the pre-trained policy, which utilizes random start and goal locations, whereas *play* data sets are generated with specific, intentionally selected goal locations. The task's reward structure is sparse, awarding points only when the robot is within a predefined proximity to the goal; otherwise, no reward is granted.

Gym-Mujoco Locomotion. In Gym-Mujoco locomotion tasks, the objective is to manage simulated robots (Walker2d, Hopper) to advance forward while minimizing energy expenditure (action norm) to ensure safe behavior. Two data generation methodologies are employed: *medium-expert* and *medium-replay*. The emphmedium-expert data sets have an equal mix of expert demonstrations and suboptimal (partially-trained) demonstrations. The emphmedium-replay data sets come from the replay buffer of a partially-trained policy. The robot's forward velocity, a control penalty, and a survival bonus all contribute to determining the task's reward.

Robosuite Robotic Manipulation. In Robosuite's robotic manipulation tasks [74], various 7-DoF simulated hand robots perform distinct tasks. Our experiments utilize environments simulated with Panda by Franka Emika, focusing on two specific tasks: lifting a cube (*lift*) and relocating a coke can from a table to a designated bin (*can*). Data collection involves inputs from either a single proficient teleoperator (*ph*) or six teleoperators with varying skill levels (*mh*). The task's reward is sparse, with further details deferred to the original paper.

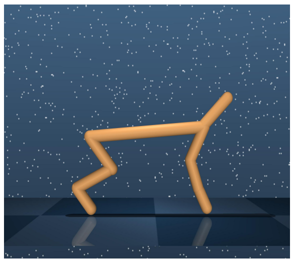
(a) Cheetah

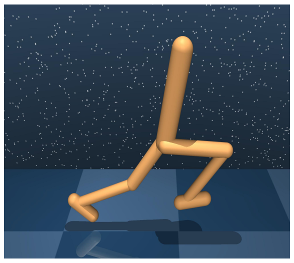
(b) Walker

(c) Quadruped

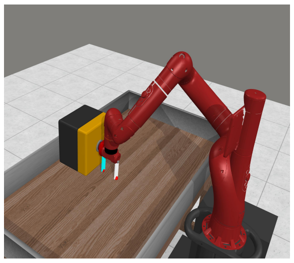
(d) Button Press

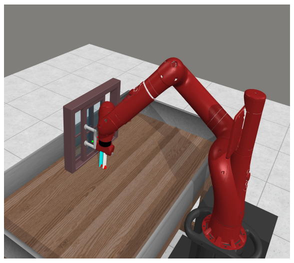
(e) Window Open

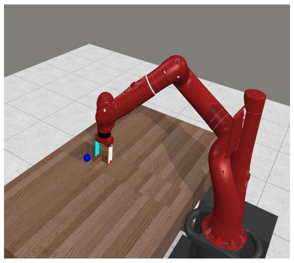
(f) Sweep Into

Figure 10: Six tasks are used for experiments. (a-c) DMControl tasks. (d-f) Meta-world tasks.

E Full Experiments

E.1 Results on Discrete Settings

A detailed introduction and visualization of the six puzzle-solving tasks from Sokoban and the three flexible environments from CraftEnv are provided in Appendix D. We selected these tasks to cover a range of complexities for our experiments. Figure 11 shows the learning curves of the average episode return for STAR and the baselines across discrete tasks. In each task, SAC, utilizing the ground-truth reward, serves as the upper performance bound. As seen in Figure 11, STAR demonstrates rapid performance gains early in training across various tasks. Remarkably, in several tasks, STAR achieves close to SAC's performance while using significantly fewer human preference labels, indicating high feedback efficiency. For example, in the Strip-shaped building task, STAR surpasses PEBBLE's average performance using only 30% of the total samples, highlighting its sample efficiency. In contrast, some baselines, affected by randomness in challenging tasks, show a decline in performance as training progresses. This underscores STAR 's robustness in maintaining performance even with fewer feedback labels. These results demonstrate that STAR substantially reduces the amount of feedback required to tackle complex tasks effectively, making it a highly efficient approach in PbRL.

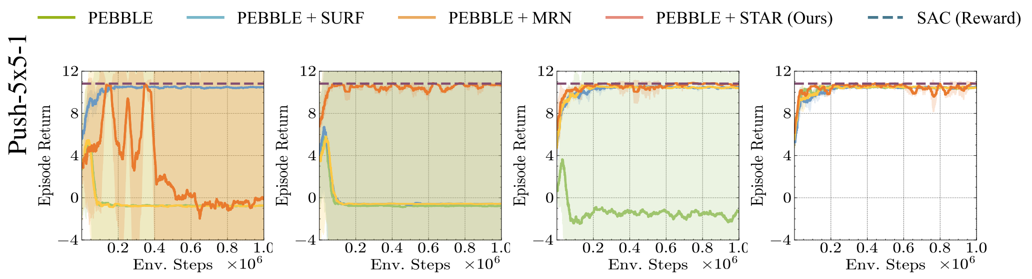

(a) feedback=50 (b) feedback=100 (c) feedback=300 (d) feedback=500

Figure 12: Training curves of all methods with varying numbers of preference labels on Push-5x5-1. The solid line presents the mean values, and the shaded area denotes the standard deviations over five runs.

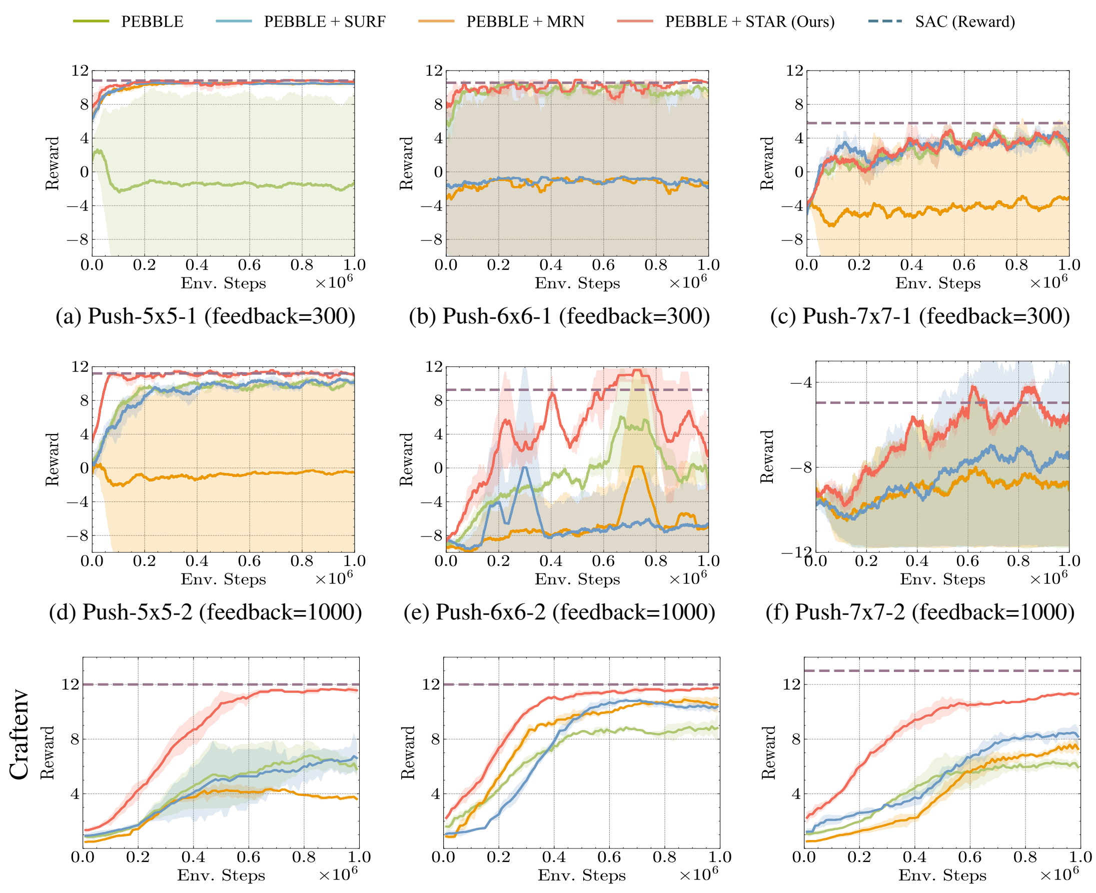

(a) Push-5x5-1 (feedback=300) (b) Push-6x6-1 (feedback=300) (c) Push-7x7-1 (feedback=300)

(d) Push-5x5-2 (feedback=1000) (e) Push-6x6-2 (feedback=1000) (f) Push-7x7-2 (feedback=1000)

(g) Strip-shaped (feedback=1000) (h) Block-shaped (feedback=1000) (i) Two-Story (feedback=1000)

Figure 11: Evaluating curves of all methods on locomotion tasks and robotic manipulation tasks. The solid line presents the mean values, while the shaded area indicates the 78% confidence interval over five runs. The red line is our method.

E.2 Ablation Studies

Impact of Preference Quantity. To assess how the amount of human preferences affects STAR 's performance, we conducted an additional experiment using varying numbers of preference labels: $N \in 50, 100, 300, 500$ on Sokoban tasks. The training curves of the average episode return for all methods are shown in Figure 12. The results reveal a clear trend: as the number of preference labels increases, STAR 's policy performance steadily improves. Notably, with sufficient preference labels, STAR approaches the performance upper bound set by SAC, highlighting its efficiency in leveraging feedback data. This trend suggests that while STAR performs well with limited preferences, providing more feedback enables it to closely match optimal performance. However, as the learning curves indicate, the rate of improvement begins to taper off at higher preference counts, suggesting diminishing returns beyond a certain threshold.

Computational Efficiency of STAR. When deploying algorithms in real-world applications, training time overhead is a critical factor. In discrete settings, we store vertices in a dictionary using hashes as keys, enabling efficient state retrieval in $\mathcal{O}(1)$ time. Additionally, updates to the graph are only required at the end of each episode, further minimizing computational overhead. In continuous settings, STAR reduces computational costs by allowing the actor to update at a lower frequency compared to traditional methods. To quantitatively assess the time overhead, Table 5 summarizes the training times (in hours) for STAR and baseline methods on Push-7x7-2 and Cheetah Run. For instance, STAR demonstrates only a slight increase in training time compared to PEBBLE, with an overhead of less than 3%. In contrast, SURF incurs a noticeable average increase of approximately 23.4% due to the additional time required for labeling samples. These results demonstrate that STAR

Table 4: Training time (hour) of various tasks. Each run is conducted using the exact same hardware environment.

Task/Methods	PEBBLE	SURF	MRN	STAR (ours)
Push-7x7-2	2.78	3.56 (+28.1%)	3.11 (+11.9%)	2.84 (**+2.2%**)
Cheetah Run	3.23	3.83 (+18.6%)	3.42 (+5.9%)	3.31 (**+2.5%**)

Table 5: Parameter search for policy regularization.

η	0	0.1	0.2	0.5	1
Quadruped Walk	790	763	728	643	620
Button Press	47	50	39	28	24
Sweep Into	55	58	52	49	48
Cheetah Run	710	713	697	579	542

maintains a favorable balance between performance and training efficiency without significantly increasing computational costs.

Sensitivity Analysis of the Parameter η. Policy regularization is a crucial component of STAR. In our experiments, we performed a parameter search for η and selected a stable value within the mid-range of the search space. The table below presents the performance of STAR on Cheetah Run for different values of η. For all experiments conducted in online settings, we set η to 6, as shown in Table 8b.

NeurIPS Paper Checklist

1. **Claims**

   Question: Do the main claims made in the abstract and introduction accurately reflect the paper's contributions and scope?

   Answer: [Yes]

   Justification: We clearly state the claims made in this paper.

   Guidelines:

   - The answer NA means that the abstract and introduction do not include the claims made in the paper.
   - The abstract and/or introduction should clearly state the claims made, including the contributions made in the paper and important assumptions and limitations. A No or NA answer to this question will not be perceived well by the reviewers.
   - The claims made should match theoretical and experimental results, and reflect how much the results can be expected to generalize to other settings.
   - It is fine to include aspirational goals as motivation as long as it is clear that these goals are not attained by the paper.

2. **Limitations**

   Question: Does the paper discuss the limitations of the work performed by the authors?

   Answer: [Yes]

   Justification: We discuss this paper's limitation and potential future work.

   Guidelines:

   - The answer NA means that the paper has no limitation while the answer No means that the paper has limitations, but those are not discussed in the paper.
   - The authors are encouraged to create a separate "Limitations" section in their paper.
   - The paper should point out any strong assumptions and how robust the results are to violations of these assumptions (e.g., independence assumptions, noiseless settings, model well-specification, asymptotic approximations only holding locally). The authors should reflect on how these assumptions might be violated in practice and what the implications would be.
   - The authors should reflect on the scope of the claims made, e.g., if the approach was only tested on a few datasets or with a few runs. In general, empirical results often depend on implicit assumptions, which should be articulated.
   - The authors should reflect on the factors that influence the performance of the approach. For example, a facial recognition algorithm may perform poorly when image resolution is low or images are taken in low lighting. Or a speech-to-text system might not be used reliably to provide closed captions for online lectures because it fails to handle technical jargon.
   - The authors should discuss the computational efficiency of the proposed algorithms and how they scale with dataset size.
   - If applicable, the authors should discuss possible limitations of their approach to address problems of privacy and fairness.
   - While the authors might fear that complete honesty about limitations might be used by reviewers as grounds for rejection, a worse outcome might be that reviewers discover limitations that aren't acknowledged in the paper. The authors should use their best judgment and recognize that individual actions in favor of transparency play an important role in developing norms that preserve the integrity of the community. Reviewers will be specifically instructed to not penalize honesty concerning limitations.

3. **Theory assumptions and proofs**

   Question: For each theoretical result, does the paper provide the full set of assumptions and a complete (and correct) proof?

   Answer: [Yes]

   Justification: We provide a detailed proof of our theorem.

   Guidelines:

   - The answer NA means that the paper does not include theoretical results.
   - All the theorems, formulas, and proofs in the paper should be numbered and cross-referenced.
   - All assumptions should be clearly stated or referenced in the statement of any theorems.
   - The proofs can either appear in the main paper or the supplemental material, but if they appear in the supplemental material, the authors are encouraged to provide a short proof sketch to provide intuition.
   - Inversely, any informal proof provided in the core of the paper should be complemented by formal proofs provided in appendix or supplemental material.
   - Theorems and Lemmas that the proof relies upon should be properly referenced.

4. **Experimental result reproducibility**

   Question: Does the paper fully disclose all the information needed to reproduce the main experimental results of the paper to the extent that it affects the main claims and/or conclusions of the paper (regardless of whether the code and data are provided or not)?

   Answer: [Yes]

   Justification: he paper provides detailed descriptions of the model architecture, training procedure, dataset, and evaluation metrics, enabling reproduction of the main results without requiring access to the code.

   Guidelines:

   - The answer NA means that the paper does not include experiments.
   - If the paper includes experiments, a No answer to this question will not be perceived well by the reviewers: Making the paper reproducible is important, regardless of whether the code and data are provided or not.
   - If the contribution is a dataset and/or model, the authors should describe the steps taken to make their results reproducible or verifiable.
   - Depending on the contribution, reproducibility can be accomplished in various ways. For example, if the contribution is a novel architecture, describing the architecture fully might suffice, or if the contribution is a specific model and empirical evaluation, it may be necessary to either make it possible for others to replicate the model with the same dataset, or provide access to the model. In general. releasing code and data is often one good way to accomplish this, but reproducibility can also be provided via detailed instructions for how to replicate the results, access to a hosted model (e.g., in the case of a large language model), releasing of a model checkpoint, or other means that are appropriate to the research performed.
   - While NeurIPS does not require releasing code, the conference does require all submissions to provide some reasonable avenue for reproducibility, which may depend on the nature of the contribution. For example
     (a) If the contribution is primarily a new algorithm, the paper should make it clear how to reproduce that algorithm.
     (b) If the contribution is primarily a new model architecture, the paper should describe the architecture clearly and fully.

(c) If the contribution is a new model (e.g., a large language model), then there should either be a way to access this model for reproducing the results or a way to reproduce the model (e.g., with an open-source dataset or instructions for how to construct the dataset).

(d) We recognize that reproducibility may be tricky in some cases, in which case authors are welcome to describe the particular way they provide for reproducibility. In the case of closed-source models, it may be that access to the model is limited in some way (e.g., to registered users), but it should be possible for other researchers to have some path to reproducing or verifying the results.

5. **Open access to data and code**

   Question: Does the paper provide open access to the data and code, with sufficient instructions to faithfully reproduce the main experimental results, as described in supplemental material?

   Answer: [Yes]

   Justification: We include source code in supplementary material.

   Guidelines:

   - The answer NA means that paper does not include experiments requiring code.
   - Please see the NeurIPS code and data submission guidelines (`https://nips.cc/public/guides/CodeSubmissionPolicy`) for more details.
   - While we encourage the release of code and data, we understand that this might not be possible, so "No" is an acceptable answer. Papers cannot be rejected simply for not including code, unless this is central to the contribution (e.g., for a new open-source benchmark).
   - The instructions should contain the exact command and environment needed to run to reproduce the results. See the NeurIPS code and data submission guidelines (`https://nips.cc/public/guides/CodeSubmissionPolicy`) for more details.
   - The authors should provide instructions on data access and preparation, including how to access the raw data, preprocessed data, intermediate data, and generated data, etc.
   - The authors should provide scripts to reproduce all experimental results for the new proposed method and baselines. If only a subset of experiments are reproducible, they should state which ones are omitted from the script and why.
   - At submission time, to preserve anonymity, the authors should release anonymized versions (if applicable).
   - Providing as much information as possible in supplemental material (appended to the paper) is recommended, but including URLs to data and code is permitted.

6. **Experimental setting/details**

   Question: Does the paper specify all the training and test details (e.g., data splits, hyperparameters, how they were chosen, type of optimizer, etc.) necessary to understand the results?

   Answer: [Yes]

   Justification: We provide the experimental setup and implementation details in Appendix.

   Guidelines:

   - The answer NA means that the paper does not include experiments.
   - The experimental setting should be presented in the core of the paper to a level of detail that is necessary to appreciate the results and make sense of them.
   - The full details can be provided either with the code, in appendix, or as supplemental material.

7. **Experiment statistical significance**

   Question: Does the paper report error bars suitably and correctly defined or other appropriate information about the statistical significance of the experiments?

   Answer: [Yes]

   Justification: We report the mean values with confidence interval.

   Guidelines:

   - The answer NA means that the paper does not include experiments.
   - The authors should answer "Yes" if the results are accompanied by error bars, confidence intervals, or statistical significance tests, at least for the experiments that support the main claims of the paper.
   - The factors of variability that the error bars are capturing should be clearly stated (for example, train/test split, initialization, random drawing of some parameter, or overall run with given experimental conditions).
   - The method for calculating the error bars should be explained (closed form formula, call to a library function, bootstrap, etc.)
   - The assumptions made should be given (e.g., Normally distributed errors).
   - It should be clear whether the error bar is the standard deviation or the standard error of the mean.
   - It is OK to report 1-sigma error bars, but one should state it. The authors should preferably report a 2-sigma error bar than state that they have a 96% CI, if the hypothesis of Normality of errors is not verified.
   - For asymmetric distributions, the authors should be careful not to show in tables or figures symmetric error bars that would yield results that are out of range (e.g. negative error rates).
   - If error bars are reported in tables or plots, The authors should explain in the text how they were calculated and reference the corresponding figures or tables in the text.

8. **Experiments compute resources**

   Question: For each experiment, does the paper provide sufficient information on the computer resources (type of compute workers, memory, time of execution) needed to reproduce the experiments?

   Answer: [No]

   Justification: We report the compute resources used in experiments.

   Guidelines:

   - The answer NA means that the paper does not include experiments.
   - The paper should indicate the type of compute workers CPU or GPU, internal cluster, or cloud provider, including relevant memory and storage.
   - The paper should provide the amount of compute required for each of the individual experimental runs as well as estimate the total compute.
   - The paper should disclose whether the full research project required more compute than the experiments reported in the paper (e.g., preliminary or failed experiments that didn't make it into the paper).

9. **Code of ethics**

   Question: Does the research conducted in the paper conform, in every respect, with the NeurIPS Code of Ethics `https://neurips.cc/public/EthicsGuidelines`?

   Answer: [Yes]

Justification: The research adheres to the NeurIPS Code of Ethics, with no ethical concerns related to data usage, human subjects, or potential misuse identified.

Guidelines:

- The answer NA means that the authors have not reviewed the NeurIPS Code of Ethics.
- If the authors answer No, they should explain the special circumstances that require a deviation from the Code of Ethics.
- The authors should make sure to preserve anonymity (e.g., if there is a special consideration due to laws or regulations in their jurisdiction).

10. **Broader impacts**

    Question: Does the paper discuss both potential positive societal impacts and negative societal impacts of the work performed?

    Answer: [Yes]

    Justification: We discuss broader impacts in Appendix.

    Guidelines:

    - The answer NA means that there is no societal impact of the work performed.
    - If the authors answer NA or No, they should explain why their work has no societal impact or why the paper does not address societal impact.
    - Examples of negative societal impacts include potential malicious or unintended uses (e.g., disinformation, generating fake profiles, surveillance), fairness considerations (e.g., deployment of technologies that could make decisions that unfairly impact specific groups), privacy considerations, and security considerations.
    - The conference expects that many papers will be foundational research and not tied to particular applications, let alone deployments. However, if there is a direct path to any negative applications, the authors should point it out. For example, it is legitimate to point out that an improvement in the quality of generative models could be used to generate deepfakes for disinformation. On the other hand, it is not needed to point out that a generic algorithm for optimizing neural networks could enable people to train models that generate Deepfakes faster.
    - The authors should consider possible harms that could arise when the technology is being used as intended and functioning correctly, harms that could arise when the technology is being used as intended but gives incorrect results, and harms following from (intentional or unintentional) misuse of the technology.
    - If there are negative societal impacts, the authors could also discuss possible mitigation strategies (e.g., gated release of models, providing defenses in addition to attacks, mechanisms for monitoring misuse, mechanisms to monitor how a system learns from feedback over time, improving the efficiency and accessibility of ML).

11. **Safeguards**

    Question: Does the paper describe safeguards that have been put in place for responsible release of data or models that have a high risk for misuse (e.g., pretrained language models, image generators, or scraped datasets)?

    Answer: [NA]

    Justification: The paper does not release models or data with high risk for misuse; thus, no special safeguards are necessary.

    Guidelines:

    - The answer NA means that the paper poses no such risks.
    - Released models that have a high risk for misuse or dual-use should be released with necessary safeguards to allow for controlled use of the model, for example by requiring

that users adhere to usage guidelines or restrictions to access the model or implementing safety filters.

- Datasets that have been scraped from the Internet could pose safety risks. The authors should describe how they avoided releasing unsafe images.
- We recognize that providing effective safeguards is challenging, and many papers do not require this, but we encourage authors to take this into account and make a best faith effort.

12. **Licenses for existing assets**

    Question: Are the creators or original owners of assets (e.g., code, data, models), used in the paper, properly credited and are the license and terms of use explicitly mentioned and properly respected?

    Answer: [NA]

    Justification: The paper does not use third-party assets that require attribution or license disclosure.

    Guidelines:

    - The answer NA means that the paper does not use existing assets.
    - The authors should cite the original paper that produced the code package or dataset.
    - The authors should state which version of the asset is used and, if possible, include a URL.
    - The name of the license (e.g., CC-BY 4.0) should be included for each asset.
    - For scraped data from a particular source (e.g., website), the copyright and terms of service of that source should be provided.
    - If assets are released, the license, copyright information, and terms of use in the package should be provided. For popular datasets, `paperswithcode.com/datasets` has curated licenses for some datasets. Their licensing guide can help determine the license of a dataset.
    - For existing datasets that are re-packaged, both the original license and the license of the derived asset (if it has changed) should be provided.
    - If this information is not available online, the authors are encouraged to reach out to the asset's creators.

13. **New assets**

    Question: Are new assets introduced in the paper well documented and is the documentation provided alongside the assets?

    Answer: [NA]

    Justification: The paper does not use third-party assets that require attribution or license disclosure.

    Guidelines:

    - The answer NA means that the paper does not release new assets.
    - Researchers should communicate the details of the dataset/code/model as part of their submissions via structured templates. This includes details about training, license, limitations, etc.
    - The paper should discuss whether and how consent was obtained from people whose asset is used.
    - At submission time, remember to anonymize your assets (if applicable). You can either create an anonymized URL or include an anonymized zip file.

14. **Crowdsourcing and research with human subjects**

Question: For crowdsourcing experiments and research with human subjects, does the paper include the full text of instructions given to participants and screenshots, if applicable, as well as details about compensation (if any)?

Answer: [NA]

Justification: This paper does not involve crowdsourcing.

Guidelines:

- The answer NA means that the paper does not involve crowdsourcing nor research with human subjects.
- Including this information in the supplemental material is fine, but if the main contribution of the paper involves human subjects, then as much detail as possible should be included in the main paper.
- According to the NeurIPS Code of Ethics, workers involved in data collection, curation, or other labor should be paid at least the minimum wage in the country of the data collector.

15. **Institutional review board (IRB) approvals or equivalent for research with human subjects**

    Question: Does the paper describe potential risks incurred by study participants, whether such risks were disclosed to the subjects, and whether Institutional Review Board (IRB) approvals (or an equivalent approval/review based on the requirements of your country or institution) were obtained?

    Answer: [NA]

    Justification: This paper does not involve crowdsourcing.

    Guidelines:

    - The answer NA means that the paper does not involve crowdsourcing nor research with human subjects.
    - Depending on the country in which research is conducted, IRB approval (or equivalent) may be required for any human subjects research. If you obtained IRB approval, you should clearly state this in the paper.
    - We recognize that the procedures for this may vary significantly between institutions and locations, and we expect authors to adhere to the NeurIPS Code of Ethics and the guidelines for their institution.
    - For initial submissions, do not include any information that would break anonymity (if applicable), such as the institution conducting the review.

16. **Declaration of LLM usage**

    Question: Does the paper describe the usage of LLMs if it is an important, original, or non-standard component of the core methods in this research? Note that if the LLM is used only for writing, editing, or formatting purposes and does not impact the core methodology, scientific rigorousness, or originality of the research, declaration is not required.

    Answer: [NA]

    Justification: The core method development in this research does not involve LLMs.

    Guidelines:

    - The answer NA means that the core method development in this research does not involve LLMs as any important, original, or non-standard components.
    - Please refer to our LLM policy (https://neurips.cc/Conferences/2025/LLM) for what should or should not be described.